Journal of Geochemical Exploration 175 (2017) 156–175

Contents lists available at ScienceDirect

Journal of Geochemical Exploration

journal homepage: www.elsevier.com/locate/gexplo

Stream sediment geochemical patterns around an ancient gold mine in the Wadi El Quleib area of the Allaqi region, south Eastern Desert of Egypt: Implications for mineral exploration and environmental studies

Mohamed Abdallah Gad Darwish

Geology Department, Faculty of Science, Aswan University, Post No. 81528 Aswan, Egypt

ARTICLE INFO

Article history:
Received 18 April 2016
Revised 2 October 2016
Accepted 18 October 2016
Available online 20 October 2016

Keywords:
Geochemical patterns
Stream sediments
Gold and heavy metal(loid)s
Economic and environmental evaluation
Wadi El Quleib area
South-eastern Desert of Egypt

ABSTRACT

The investigation of geochemical patterns in stream sediments around the newly discovered ancient gold mine in the Wadi El Quleib area is aimed at economic evaluation and environmental assessment of catchment sediments. For these reasons, forty stream sediment's composite samples were collected from the area covered by the metamorphosed ultramafic and their derivatives, volcanogenic metasediments, granitoid plutons, sand stones, and unconsolidated sediments. Fifty three chemical elements were analyzed using inductively coupled plasma–mass spectrometry. They were processed using various mathematical computations, graphical plots, and mapping techniques. The results revealed that the multiple populations within data set were caused by natural and ancient mining activities. Both geogenic and anthropogenic sources could influence on the dispersion of the elements of interest in the stream sediments. Despite sediments' materials were predominantly generated from metabasic and ultramafic provenance rather than mixed and flesic sources, and the area may have been subjected to more than one weathering cycle, they did not follow the sedimentary sorting and recycling trend. The lack of Au content and the negative correlation of Au with other elements are due to ancient human works and thus, the combined elements Ag + As, Ag + Hg, and Ag + Hg + As are considered the pathfinder for Au mineralization. The metamorphosed ultramafic and their derivatives, volcanogenic metasediments and their thrust contact host Au-mineralization, Cr-mineralization, and Ni-bearing minerals. Environmentally, the low values of contamination degrees and potential ecological risk indices of heavy metal(loid)s indicated that the sediment materials are good in quality and possess no actual hazard to human health. In general, the study area is more promising for Au mineralization and accepted as safe environment for the urban renewal purposes and land-use management in the future.

1. Introduction

The primary geochemical patterns in rocks were formed during different geological processes; they can be transmitted during weathering to various surficial materials (Xuejing and Binchuan, 1993). Likewise, anomalous and background geochemical patterns are associated with different geological processes whereby anomalous geochemical patterns may be due to mineralization; background geochemical patterns may be due to regional geological process (Cao and Cheng, 2012). The recognition of geochemical pattern has been used over many years in exploration geochemistry and environmental purposes. Since the 1970s, geochemical pattern recognition techniques have been applied to recognize geological and the economic mineral resource informations hidden in geochemical data (Briggs, 1978; Castillo-Munoz and Howarth, 1976; Collyer and Merriam, 1973; Gustavsson and Bjorklund, 1976; Howarth, 1973). They used also to investigate the relations between regional geochemical patterns and large ore deposits (Xie et al., 2004), and recognition of polluted sites and their types (Hanesch et al., 2001). In the secondary environment such as stream sediments, the local geochemical patterns are related to multiple factors such as natural, anthropogenic, or both sources (Chipres et al., 2009). Although it is well established that background geochemical patterns in stream sediments are generally depending on drainage basin geology, little is known about the effects of watershed disturbance on such patterns (Christie and Fletcher, 1999).

According to Cohen et al. (1999), stream sediments are commonly the principal sampling medium in regional reconnaissance geochemical surveys; they are used extensively to characterize the general geochemistry of catchments (baseline analysis) and isolate areas with a typical geochemistry (anomaly detection); Crock et al. (1992) and Darnley (1997), a geochemical investigation based exclusively on systematic sampling will detect areas enriched in certain trace elements and run into difficulties in discerning whether the anomaly is geogenic or

E-mail address: mohamed.darwish26@yahoo.com.

http://dx.doi.org/10.1016/j.gexplo.2016.10.010
0375-6742/

anthropogenic; Cicchella et al. (2013), the robustness of geochemical patterns is produced from low-density surveys; Smith and Reimann (2008), summarized several examples of existing low-density geochemical mapping projects that show the robustness of the map patterns, and the relationship between those patterns and processes acting at these large scales. Consequently, it is the better to apply composite sampling technique that is effective for this purpose because it is whereby multiple temporally or spatially discrete media samples are combined, thoroughly homogenized, and treated as a single sample (Correll, 2001; El Baz and Nayak, 2004; Splitstone, 2001). Additionally, the composite sampling can improve spatial or temporal representations of the data by reducing the number of analyzed samples, analytical costs, and the local, in space or time, variability (Cicchella et al., 2013).

The geochemical data of stream sediment sampling provide efficient guides for identifying regional geochemical patterns and locating areas with high potential for further mineral exploration (Abdolmaleki et al., 2014). As well, they are used for a range of purposes, including land-use planning and agricultural development, and environmental assessment of both natural and anthropogenic hazards (Appleton and Ridgway, 1992; Plant et al., 2001). Stream sediments, soils, and waters have been used in many countries across different scales for regional geochemical mapping (e.g. Darnley, 1990; BGS, 1990; Reimann et al., 1998; Rice, 1999; Key et al., 2004; Salminen et al., 2005; Johnson et al., 2005). In post-mining and industrialized areas, sediments and soil geochemical mapping is now primarily used for environmental purposes, including separation of natural from anthropogenic sources of metals and organics, evaluation of soils for agricultural purposes, environmental management, medical geochemistry and land uses classification (Tan, 1989; Plant et al., 2000, 2003; Reimann et al., 2011). In addition, it is used for establishing the environmental levels of various heavy metals for outlining areas of potential toxicity (Navas and Machĭn, 2002), determine contamination processes, and contribute toward the improvement of the environment (Ohta et al., 2007). Moreover, the geochemical mapping was originally directed toward mineral exploration (Garrett et al., 2008) in order to illustrate natural geochemical background variation (Ohta et al., 2007), define lateral surface distribution of the elements, and identify geochemical anomalies that are indicative of mineralization and contaminant sources (van Helvoort et al., 2005).

In the case of ancient gold mines, stream sediment geochemical patterns might be modified due to old anthropogenic activities of surface mining works (such as tailing material, disposing of wastes onto the sediments, atmosphere .....etc.). This leads to a distinct local input event superimposed on the natural background geochemical patterns. In the study area, during the field works and trips, the author found out the aspects of old traditional ore processing and mining activities for gold. They are represented by few scattered heaps and dams of tailing materials, dispersed ore dumps, overturned, pitted and trenched streambed sediments, stone mills with grinding stones, and antique ruins. These aspects are similar to those existed in the ancient gold mines in the south-Eastern Desert of Egypt, especially in Allaqi region. Due to the mentioned evidences were unknown and not mentioned in all published and non-published literatures, and Egyptian records, the present disused and abandoned gold-mining location detected by the author is considered as newly discovered ancient gold mine in the Wadi El Quleib area.

According to the rate of urbanization in south Egypt, especially in the Wadi Allaqi region, there are no records of Au mineralization and old mining works, and no information available on both secondary geochemical pattern and environmental assessment of the study area. There is a necessity to carry out the economic evaluation of stream sediments and assess the influence of contributing inputs of the former human activities on the sediments' materials around the discovered gold mine. Therefore, the present paper aims for (1) Estimating geochemical baseline levels of trace elements. (2) Delineating geochemical patterns and their pathfinder elements to detect Au mineralization and potentially toxic elements. (3) Identifying processes that produced geochemical patterns and evaluate different contributing sources. (4) Outlining sites of interest that must be considered in making decisions of optimal exploration target and land-use purposes in the future.

2. Study area

The Wadi El-Quleib area is located between 33° 09′ E and 33° 27′ E longitude and 22° 40′ N and 22° 51′ N latitude. It is existed in south-Eastern Desert of Egypt (Fig. 1a) with a total surface area of about 317.34 km^2. The study area is concerned with the Wadi El-Quleib, which is a dry valley with a length of about 14 km, intersecting the Wadi Allaqi. The entrance of the Wadi El Quleib is lying at intersection of latitude 22° 46′ 09″ N and longitude 33° 13′ 02″ E (179 m a.s.l.), and being approximately 220 km southeast from the Aswan city. It is also characterized by granititic pluton, “dubbed Deneibit El Quleib”, which is located in the southeastern corner of the study area (339 m a.s.l.). The Wadi El Quleib and its tributaries were drained the study area, forming dendritic drainage network with average width varies from 10 m at the upstream to 320 m at the downstream. The drainage pattern was filled with stream sediment materials that were mainly derived by weathering activities acting on the surrounding and underlying various lithologic units. The average thickness of streambed sediment is varying from 40 cm at the upper streams (222 m a.s.l.) to >3 m at the middle stream (193 m a.s.l.) and the downstream (179 m a.s.l.). The difference in elevation reflects the gentle slope in the Wadi El Quleib floor.

The climate is typical extreme arid type with scarce rainfall, hot summer and cold winter, and average temperature exceeds 45 °C in summer and around 15 °C in winter. July and August are the hottest months during the summer while, January and February are the coldest months during the winter. Although the rainfall is rare, sometimes the thunderstorms with heavy rain took place for a short duration varying from few ten minutes to few hours, forming annual torrents, especially between October to January. These rains charged with poorly sorted sediments of weathered bedrock and desert soils have poured and deposited their loads in the drainage pattern within the Wadi El Quleib area. Besides thunderstorms with heavy rains, windblown sand and dust-laden wind could bring a small amount of load materials from surrounding country rocks and their environs to the study area. Hence, the stream sediments' availability was high and their transportation was generally associated with the mentioned erosion activities.

Despite the climatic condition is arid and rainfall is rareness, some plants are growing over stream sediments of the study area, and they increased toward downstream due to the water surface of the Lake Nasser is near to the entrance of the Wadi El Quleib. The vegetation cover is represented by some trees and shrubs such as *Acacia ehrenbergiana*, *Acacia raddiana*, *Balanities aegyptiaca Tamarix nilotica*, *Aerva javanica*, *Pulicaria crispa*, *Fagonia Indica*, *Cynodon daclyton*, *Citrullus colocynthis* and *Senna Alexandrina*. Most of the mentioned plants are regarded as natural grazing for poultry, goat, sheep, gazelle, donkeys and camels; these animals (except donkeys) are the main sources of meat for the Bedouins living in the Wadi Allaqi and peoples living in Aswan City. Based on the field monitoring in the study area, there are neither rapid developments arrived nor covered by land used (e.g., cultivable land, industry and settlement). Even so, the ancient mining and ore processing activities monitored beside and near an abandoned gold mine were dependent on the stream sediment materials and surface mineralized zones within the drainage basin of the study area. Despite the previously mentioned old working is presented, there are no huge mining operations were observed near the surface of country rocks.

3. Geology of the area

Some literatures described the geology, structures and geochemistry of country rocks from the Wadi El Quleib area and its environs; they have been published by Ragab and El Shimy (1994), El Shimy (1996),

Rashawan and Schleicher (1996), Abdel Hamid (1997), Noweir and El Amawy (1999), Fawzy et al. (2000), Noweir et al. (2000), Saleh and Abd El Wahed (2001), Ahmed (2002), and El Afandy et al. (2007). The surface geology of the area belongs to the Arabian-Nubian Shield of Neoproterozoic age, and represents the crystalline basement rocks that have been affected by deformation and metamorphism during the Pan African Orogeny. These rocks have been overlain by sedimentary rocks, especially in the western part of the study area (Fig. 1b). Overall, the country rocks can be grouped into four main lithologic units: (1) metamorphosed ultramafic and their derivatives, (2) volcanogenic metasediments, (3) calc-alkaline intrusive granitoid plutons, and (4) Nubian sand stones of Cretaceous age and Quaternary sediments.

The metamorphosed ultramafic and their derivatives are represented by serpentinites, meta-amphibolites, metapyroxenites, and talc-carbonate and related schists. They were tectonically thrust over volcanogenic metasediments; some fragments and lens-like bodies of these mentioned rocks were enclosed in volcanogenic metasediments unit. Along the thrust contact, small veins and veinlets of asbestos, magnesite and talc and talc carbonates have been formed. Volcanogenic meatsediments composed of metamudsones, metasiltsones, metagraywackes, metatuffs (fine grained tuffaceous metadacite, fine crystal metatuffs, lapilli-crystal and coarse crystal acidic metatuffs), biotite and muscovite schists, and marble bands. The emplacement of ophiolitic assemblage was due to SE-NW obduction; the accretion related thrusts led to form large parallel faults (Church, 1988). The previous two lithologic units were metamorphosed in varying grades ranging from green schist to low amphibolite facies (Noweir et al., 2000), and subsequently they were intruded by intrusive calc alkaline plutonic granitoid rocks. The latter include: (A) Umm Shakait granitoid which is located in southwestern part is older and composed of quartz diorite suites (El Afandy et al., 2007). (B) Deneibet El Quleib granitoid (4.4 × 4.2 km) is found in southeastern corner and represents younger granites varying in composition from granodiorite to adamellite and granite, which are peraluminous, calc alkaline to weakly alkaline and of I-type (Noweir and El Amawy, 1999; El-Sayed and Nisr, 1999). (C) Heisurbah granitoid appears in the northeastern part on the study area, and is regarded as older granitoid possessing granodiorite composition (El Afandy et al., 2007). (D) granitoid pluton that is exposed in northern part of the mapped area was classified as alkali granite (Saleh and Abd El Wahed, 2001).

The Wadi El Quleib area has been dissected by a number of faults that are mainly trending in NNE-SSW and ENE-WSW directions, while fewer numbers trending NNW-SSE and WNW-ESE directions (Fig. 1b). Lineations (L1, L2 and L3), and foliation planes (S1, S2, and S3) are related to the first, second, and third phases of deformations (El Afandy et al., 2007). To be brief, the study area was affected by at least three phases of ductile deformation (D1–D3) (Fawzy et al., 2000): the first and second deformations (D1 and D2) were formed pre-granite intrusion, whereas the third deformation (D3) was formed syn-granite intrusion (Noweir and El Amawy, 1999).

The literatures carried out by Noweir and El Amawy (1999), Noweir et al. (2000), Saleh and Abd El Wahed (2001), Ahmed (2002), and El Afandy et al. (2007) revealed that the previously mentioned granitoids had average concentrations of some trace elements (such as, Ba, Ce, Ga, La, Nb, Ni, Rb, Sr, Th, U, Y, and Zr) in the crustal abundance level. While, Co, Cr, Cu, Ni, Pb, and Y are only elevated in metamorphosed ultramafic and their derivatives, and volcanogenic metasediments units.

The sedimentary rocks appeared in the western part within the study area are represented by Nubian sandstones of Cretaceous age. Finally, the unconsolidated sediments of Quaternary age include both recent sediments capped few parts of the country rocks, and the stream sediments filling the Wadi El Quleib drainage basin and the Wadi Allaqi. All sediment materials are poorly sorted, generated by the effects of weathering processes on surrounding lithologic units, predominantly composed of boulder, cobble, gravel, sand, silt and clay fractions. These sediment materials were extensively screened for gold by ancient mine workers in the past times.

4. Methodology

4.1. Sampling method and preparation of samples

The sampling procedures were carried out in two weeks of February 2013, and two weeks in August 2013 because the drainage basin was dry. In order to perform the economic evaluation and environmental assessment of Quaternary stream sediments, a series of forty composite samples was collected from forty sampling stations (1 sample/7.93 km^2), covering the entire drainage basin. The traditional manual sampling tools were specifically grub hoe, mattock, shovel, garden rake, hand trowel, and scoop. Each composite sample represented one sampling station was generated from five sampling points over an area of nearly 2 m × 10 m perpendicular to the strike of the stream at a depth of 30–50 cm. The mentioned depth was chosen to avoid any disturbances caused by tailing materials, manure, dry plant remains, track path, and wind blown sand and dust. The distance between sampling stations was not fixed depending on the topography, tributaries and lithology of drainage pattern. After removing the boulders, cobbles, coarse gravels, the sediment materials were dry sieved in the field using a minus 1 cm stainless steel sieve and then through a minus1 mm stainless steel sieve, until reach of about 10 kg at each sample station. The generated samples were sealed in clean labeled polyethylene bags and transported to the laboratory for further treatment.

In the laboratory, each sample (ca. 10 kg of minus 1 mm) was reduced to 500 g using the cone and quarter method, and air dried in the room temperature (ca. 40 °C) for 72 h to ensure their dryness. Subsequently, 100 g produced by cone and quarter method was ground by electro-mechanical agate mill machine to obtain the fine homogeneous powder and then, passed through 63 μm sieve to get suitable particle size for the chemical analysis. In order to avoid a probable metal rust contamination during samples' collection at the field and their preparation in the laboratory, the sampling tools, pan, spoon, and spatula were made of stainless steel. Moreover, all mentioned tools and agate mortar were cleaned and rinsed with the fresh water followed by Milli-Q water; they were air dried after performing each sample in order to prevent the potential contamination.

4.2. Analytic method of samples and quality control

Prior to perform the chemical analysis, a portion of approximately 16 g of each prepared sediment sample (minus 63 μm) was re-dried at temperature of 40 °C to avoid volatile loss, and sealed in pre-numbered small polyethylene sacks. Subsequently, all set samples were sent to the ACME Analytical Laboratories Ltd. (Vancouver, Canada); accredited under ISO 9001 and 17,025 documentation for their chemical analysis. A suit of 53 chemical elements (Ag, Al, As, Au, B, Ba, Be, Bi, Ca, Cd, Ce, Co, Cr, Cs, Cu, Fe, Ga, Ge, Hf, Hg, In, K, La, Li, Mg, Mn, Mo, Na, Nb, Ni, P, Pb, Pd, Pt, Rb, Re, S, Sb, Sc, Se, Sn, Sr, Ta, Te, Th, Ti, Tl, U, V, W, Y, Zn, and Zr) were determined according to standard method codes AQ251-EXT, using Inductively Coupled Plasma Mass Spectrometry (ICP-MS, model Perkin Elmer ELAN 6000, USA) and following an aqua regia digestion (1 h, 95 °C) on a 15 g aliquot.

The quality control, accuracy and analytical precision were performed applying instrumental calibration, and analyses of certified standard reference materials, internal reference materials (STD-DS 10 and STD-OXC109; provided by ACME Analytical Laboratory), blank samples, and replicate samples in each analytical set. Moreover, 10% of the duplicate samples were re-analyzed and showed that all chemical elements in blank solutions were below their corresponding lower detection limits. According to the assessment of data quality results, the concentration measurement accuracy was estimated at ±5% for all the analyzed elements.

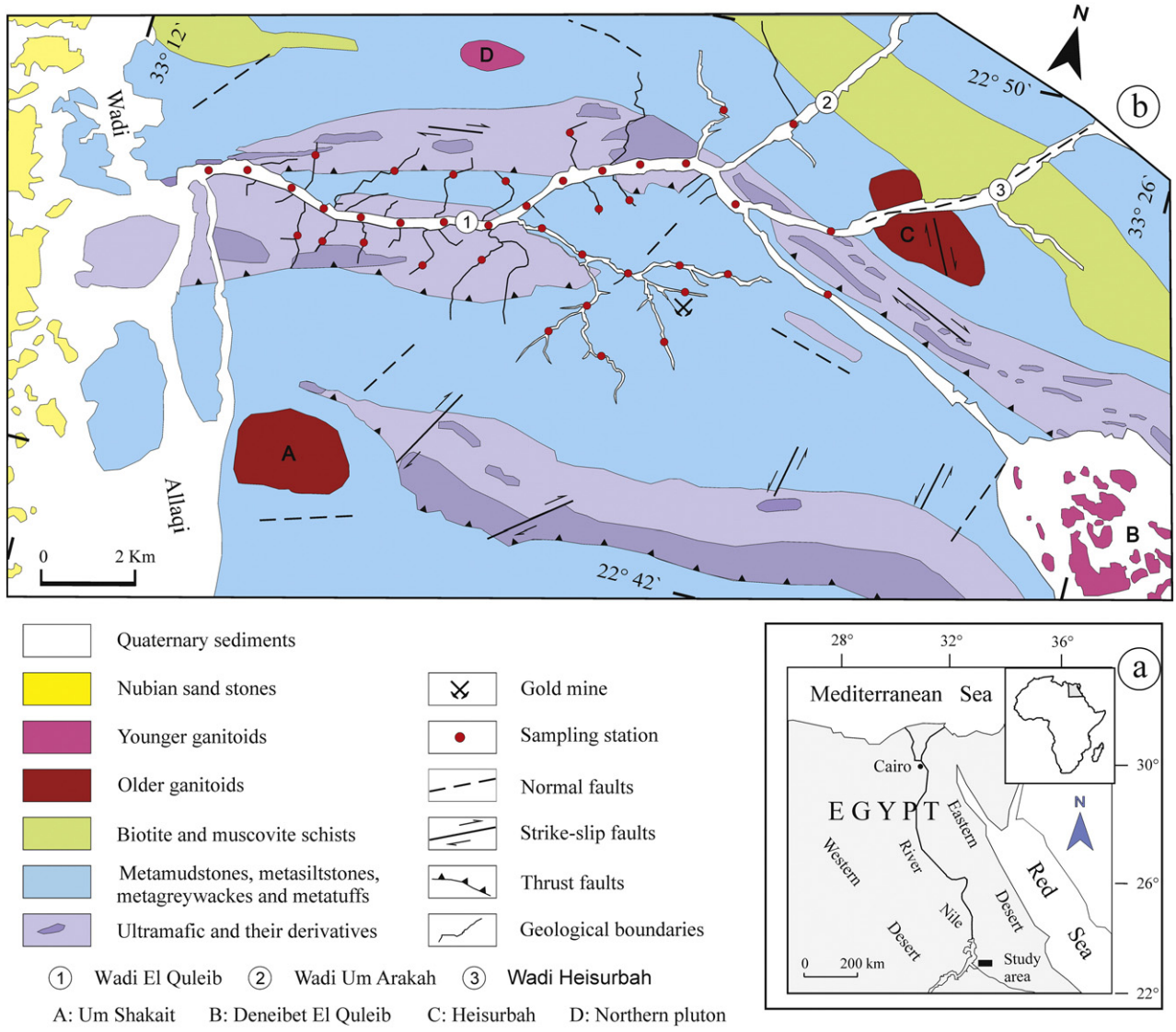

Fig. 1. Geological context of the Wadi El Quleib area, Allaqi region, south-Eastern Desert of Egypt. (a) Sketch map showing location of the study area; (b) Geological map (modified after Noweir et al., 2000 and El Afandy et al., 2007) with stream sediment sampling stations represented by red circles.

Sensitivity in the sense of a lower limit of detection was adequate for 43 out of 53 analyzed chemical elements. Ten elements were removed from further statistical analysis because their contents in the majority of analyzed samples were below the lower detection limit of the analytical method. These elements are: Ge (62.5%), In (57.5%), Pd (97.5%), Pt (90%), Re (87.5%), S (97.5%), Se (87.5%), Ta (100%), Te (77.5%), and W (80%). In contrast, concentrations of Au (10%) and Hg (11%) were below the lower limit of detection (0.2 and 5 ppb respectively) and therefore, these concentrations were replaced by half of their detection limit, as suggested by Chapman (1996).

5. Data processing requirement

5.1. Statistical analysis

A range of common statistical techniques have been applied in the present study; they include univariate, bivariate and multivariate analyses in order to explore and investigate the data structure, trends and variables' associations within the geochemical data for better understanding of elemental relationship and the factors controlling the stream sediment geochemistry. Statistical analyses were performed in accordance with the suggestion of Chandrajith et al. (2001), who mentioned that the geochemical compositions of the selected fractions were interpreted using statistical techniques, which will help in the recognition of any additional subtle, though important geochemical patterns that may exist within the study area.

5.1.1. Descriptive statistics

At the outset, the geochemical data were mathematically treated to obtain the descriptive statistics that used to assess the overall features of the element concentrations within the examined data. The descriptive statistics in the present study have been calculated for the analyzed forty three elements and generated the following statistical parameters: minimum, median, mean, maximum, geometric mean, and mode for the central tendency measurement; median and mean absolute deviation, standard deviation, variance, and variation coefficient for the statistical dispersion measurement. Furthermore, the geochemical data were subjected to normality test called “Shapiro-Wilk (S–W) test” for investigation the statistical distribution of data set applying the null hypothesis; they were also tested for asymmetry and tailedness using skewness and kurtosis, respectively. Undoubtedly, the mentioned parameters are helpful for comparing data sets, summarizing their results and facilitating and supporting their interpretation.

Table 1
Summarized statistics and the average contents in the upper continental crust (UCC) of the chemical elements distributed in the stream sediment sampling stations (N = 40) from the Wadi El Quleib area of the Allaqi region, south Eastern Desert of Egypt.

Element	Unit	Minimum	Median	Mean	Maximum	Geometric mean	Mode	MAD	Mean absolute deviation	Standard deviation	Variance	Coefficient of variation	Skewness	Kurtosis	(K–S p)	UCC
Al	%	1.2	1.61	1.74	2.6	1.70	1.2	0.25	0.33	0.41	0.16	0.23	0.78	−0.39	0.005	8.04
Ca	%	0.63	1.105	1.26	2.26	1.20	0.81	0.27	0.34	0.41	0.16	0.32	0.75	−0.25	0.013	3
Fe	%	1.42	2.05	2.18	3.36	2.13	1.77	0.26	0.37	0.48	0.23	0.22	0.77	−0.11	0.012	3.5
K	%	0.17	0.28	0.30	0.7	0.29	0.32	0.04	0.07	0.10	0.01	0.34	2.12	5.54	0.000	2.8
Mg	%	0.56	0.82	0.87	1.49	0.85	0.85	0.12	0.18	0.23	0.06	0.27	1.18	0.88	0.001	1.33
Mn	ppm	260	361.5	392.7	603	382.15	260	41.50	76.65	96.33	9280	0.25	0.89	−0.24	0.001	600
Na	%	0.033	0.055	0.07	0.762	0.06	0.062	0.01	0.04	0.11	0.01	1.57	6.20	38.95	0.000	2.89
P	%	0.03	0.039	0.04	0.076	0.04	0.037	0.00	0.01	0.01	0.00	0.24	1.75	3.00	0.000	0.07
Ti	%	0.083	0.098	0.11	0.184	0.11	0.094	0.01	0.02	0.02	0.00	0.22	1.57	2.19	0.000	0.3
Ag	ppb	20	28	33.90	89	31.94	28	5.00	9.77	13.71	187.9	0.40	2.19	5.89	0.000	50
As	ppm	0.9	1.9	2.24	4.7	2.09	1.8	0.40	0.68	0.86	0.75	0.39	1.10	0.65	0.001	1.5
Au	ppb	0.1	0.6	0.89	7	0.55	0.5	0.40	0.63	1.17	1.36	1.31	4.03	19.65	0.000	1.8
B	ppm	2	3	3.68	6	3.51	3	1.00	0.94	1.12	1.25	0.30	0.58	−0.48	0.000	15
Ba	ppm	57.5	81.05	86.24	163.4	83.63	68.7	12.40	17.69	23.38	546.5	0.27	1.53	2.58	0.000	550
Be	ppm	0.2	0.4	0.43	0.9	0.41	0.4	0.10	0.10	0.13	0.02	0.31	1.29	3.04	0.000	3
Bi	ppm	0.03	0.06	0.06	0.14	0.06	0.04	0.02	0.02	0.02	0.00	0.38	1.18	1.72	0.002	0.127
Cd	ppm	0.05	0.08	0.09	0.15	0.09	0.08	0.02	0.02	0.02	0.00	0.26	0.42	−0.32	0.065	0.098
Ce	ppm	19.3	27.05	27.90	54.3	27.31	29.1	2.65	4.18	6.40	40.98	0.23	2.14	7.04	0.000	64
Co	ppm	6.4	9.9	10.91	19.6	10.55	8.9	1.45	2.29	3.10	9.59	0.28	1.35	1.54	0.000	10
Cr	ppm	27.3	40.3	46.60	89.8	44.44	36	7.55	12.39	15.46	239.0	0.33	1.16	0.81	0.001	35
Cs	ppm	0.4	0.59	0.63	1.43	0.61	0.45	0.09	0.14	0.21	0.05	0.34	2.12	5.45	0.000	3.7
Cu	ppm	12.11	18.185	20.24	40.49	19.43	–	2.37	4.65	6.48	42.00	0.32	1.65	2.38	0.000	25
Ga	ppm	3.3	4.7	5.02	8.3	4.91	4.2	0.65	0.87	1.09	1.20	0.22	1.04	0.90	0.009	17
Hf	ppm	0.16	0.205	0.21	0.31	0.21	0.23	0.03	0.03	0.03	0.00	0.15	0.87	1.21	0.028	5.8
Hg	ppb	2.5	9	9.99	25	8.14	2.5	4.00	4.71	6.08	36.92	0.61	0.82	0.17	0.008	46
La	ppm	9.7	13.2	13.60	25.8	13.30	13.2	1.45	2.13	3.18	10.10	0.23	1.97	5.37	0.000	30
Li	ppm	6.5	9.25	10.07	19.1	9.73	7.8	1.45	2.19	2.88	8.29	0.29	1.52	2.72	0.000	20
Mo	ppm	0.25	0.395	0.42	0.72	0.41	0.37	0.06	0.08	0.10	0.01	0.24	0.98	0.82	0.014	1.5
Nb	ppm	0.08	0.165	0.17	0.31	0.16	0.18	0.03	0.04	0.05	0.00	0.31	0.47	0.23	0.491	25
Ni	ppm	19.6	28.5	33.01	60.4	31.59	27.1	3.70	8.39	10.60	112.3	0.32	1.18	0.56	0.000	20
Pb	ppm	2.74	4.09	4.36	8.7	4.21	4.09	0.70	0.95	1.29	1.66	0.30	1.61	3.14	0.000	20
Rb	ppm	7.5	12.6	13.74	31.1	13.10	9.9	2.20	3.39	4.81	23.16	0.35	1.91	4.37	0.000	112
Sb	ppm	0.05	0.07	0.07	0.13	0.07	0.06	0.01	0.01	0.02	0.00	0.23	1.03	1.41	0.001	0.2
Sc	ppm	4.1	5.2	5.49	7.1	5.44	5.1	0.40	0.62	0.77	0.59	0.14	0.75	−0.41	0.002	11
Sn	ppm	0.3	0.5	0.54	1	0.52	0.5	0.10	0.09	0.12	0.02	0.23	1.38	4.21	0.000	5.5
Sr	ppm	27.8	35.85	37.76	56.7	37.12	32.5	4.75	5.91	7.31	53.39	0.19	0.86	0.27	0.018	350
Th	ppm	2.7	3.9	4.10	7.3	4.00	3.4	0.50	0.70	0.96	0.91	0.23	1.49	2.83	0.001	10.7
Tl	ppm	0.03	0.06	0.07	0.18	0.07	0.06	0.01	0.02	0.03	0.00	0.36	2.37	8.23	0.000	0.75
U	ppm	0.42	0.55	0.56	1.13	0.55	0.55	0.06	0.07	0.12	0.01	0.21	2.98	13.42	0.000	2.8
V	ppm	31	45.5	47.95	76	46.94	45	5.50	7.79	10.44	108.9	0.22	1.02	0.66	0.005	60
Y	ppm	6.49	8.505	8.77	13.12	8.69	8.41	0.63	0.89	1.26	1.58	0.14	1.39	2.97	0.002	22
Zn	ppm	26.3	36.8	38.93	67.1	38.14	36.4	4.05	6.27	8.43	71.02	0.22	1.35	2.20	0.001	71
Zr	ppm	5.5	7.25	7.59	11.4	7.50	7.2	0.75	0.98	1.23	1.50	0.16	0.87	0.99	0.058	190

N: number of sampling stations; MAD: median absolute deviation; (S–W p): significance levels of the Shapiro-Wilk test; UCC: upper continental crust (Taylor and McLennan, 1995) while Hg after Beus and Grigorian (1977); Asterisk: moderate contamination factor.

5.1.2. Exploratory data analysis (EDA)

EDA was applied in the present study because it is an appropriate technique for identifying anthropogenic influences and determining the geogenic concentration or geochemical background value of soil (Zhou and Xia, 2010); the latter value will serve as a reference to assess the soil contamination by toxic elements (Khalil et al., 2013). The EDA technique in the current manuscript is represented by box and whiskers plot to look for various intervals of poisonous element concentrations, which imply likely the presence of different processes or multiple populations (Zhou and Xia, 2010).

5.1.3. Spearman–rho correlation coefficient (rs)

The degree of geochemical association for the interested elements and the relationship between paired elements were assessed by a non-parametric Spearman–rho correlation coefficient (r_s), which represents the bivariate analysis of the examined geochemical data. The choice of Spearman-rho correlation is due to its less sensitive to outliers; it does not assume a linear relationship between variables. The inter-element relationships can provide interesting information on heavy metal sources and pathways (Dragovic et al., 2008; Manta et al., 2002).

5.1.4. Cluster analysis (CA) and principal component analysis (PCA)

Multivariate statistical analysis has seen widespread application in the fields of mineral exploration and environmental protection; they are used for re-interpretation and understanding the geochemical patterns of arid desert terrains, and giving the helpful information for further exploration in similar terrains (Lin et al., 2014). In this regards, R-mode cluster analysis has been performed to measure the divergence, and classify the examined elements existed in the geochemical data into new groups named as clusters. Besides, it enables to discriminate various groups of heavy metal(loid)s as tracers of a natural or an anthropogenic source (Martínez et al., 2007). In this study, hierarchical cluster analysis generated by Ward's method and Euclidean distance was chosen after assessing the different hierarchical agglomerate clustering combinations. Principal component analysis (PCA) has also been applied, since it is widely used in geochemical studies to identify the relationship and the origin of trace elements (Lu et al., 2010) and also to

reduce the data dimension sets to lower dimensions by identifying independent factors and associations among groups of observed variables (Davis et al., 2009). The values of the factor matrix can be improved by using the Varimax rotation method, which maximizes factor variance (Kaiser, 1958).

5.2. Major elements and weathering

The bulk chemical changes that take place during weathering have been used to quantify the weathering history of sedimentary rocks, primarily to understand past climatic conditions (Nesbitt et al., 1980; Nesbitt and Young, 1982, 1984). For these reasons, three chemical weathering indices have been used: CIA (chemical index of alteration) proposed by Nesbitt and Young (1982), CIW (chemical index of weathering) after Harnois (1988), and ICV (index of compositional variation) based on Cox et al. (1995).

The CIA has been established as a general guide to the degree of weathering and its intensity. It can be calculated based on molecular proportions employing the following formula:

$$CIA = [Al_2O_3/(Al_2O_3 + K_2O + Na_2O + CaO^*)] \times 100 \quad (1)$$

In this respect, kaolinite and chlorite have CIA values of nearly 100; average shales have CIA values ranging from 70 to 75 (Nesbitt and Young, 1982); residual clays possess CIA values between 85 and 100 (Taylor and McLennan, 1985); and un-weathered igneous rocks have CIA values of 50 or less (McLennan et al., 1993). According to Nesbitt and Young (1984), the intensive chemical weathering in the source areas is represented by the high values of CIA ranging from 76 to 100.

The CIW can be performed using the following formula:

$$CIW = [Al_2O_3/(Al_2O_3 + CaO^* + Na_2O)] \times 100 \quad (2)$$

In addition to CIA and CIW, the ICV has been applied to support the calculation results of both CIA and CIW; it can be computed applying the following formula:

$$ICV = [Fe_2O_3 + K_2O + Na_2O + CaO + MgO + MnO + TiO_2]/Al_2O_3 \quad (3)$$

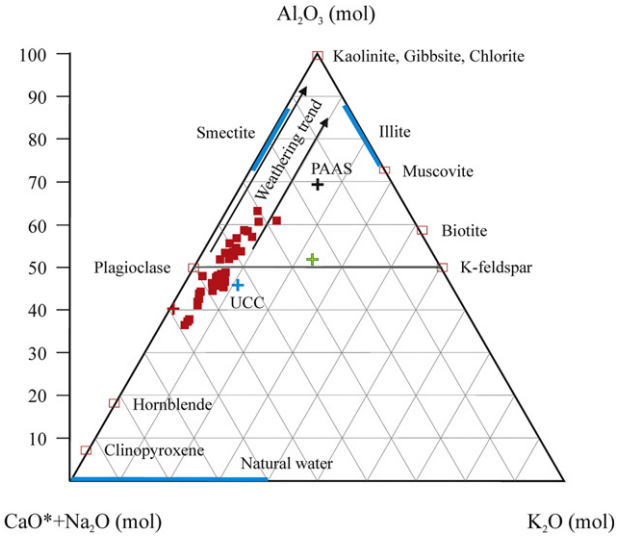

Fig. 2. Ternary plot of Al_2O_3–(CaO^* + Na2O)–K2O (A–CN–K) for the stream sediment data of the Wadi El Quleib area: selected rock and mineral compositions, and weathering trends, proposed by Nesbitt and Young (1982, 1984, 1989), are given with colored crosses, red is average N-MORB (Sun and McDonough, 1989); green is average granite (Nockolds, 1954); blue is average upper continental crust "UCC", and black is average post-Archean Australian shale "PAAS" (after Taylor and McLennan, 1985) are shown for comparison.

Table 2
Summarized statistics of calculated CIA, CIW, ICV, and K_2O/Al_2O_3 ratio distributed in the stream sediment sampling stations (N = 40) from the Wadi El Quleib area of the Allaqi region, south Eastern Desert of Egypt.

	Minimum	Mean	Median	Maximum	Standard deviation
CIA	36.13	48.75	47.32	62.81	6.55
CIW	37.88	51.88	50.25	68.20	7.39
ICV	1.68	2.15	2.16	2.54	0.20
K_2O/Al_2O_3	0.05	0.11	0.11	0.17	0.03

N: number of sampling stations; CIA: chemical index of alteration (Nesbitt and Young, 1982); CIW: chemical index of weathering (Harnois, 1988); ICV: index of compositional variation (Cox et al., 1995).

where, CaO^* in Eqs. (1) and (2) is the amount of CaO integrated only in silicate minerals. Since the CO_2 data of the present study are not available, CaO^* was corrected for calcium residing in carbonates and phosphates based on McLennan (1993) method.

5.3. Trace elements and provenance

Certain elemental ratios are regarded as characteristic of the provenance and sedimentary sorting and recycling of stream sediments. It is known that the immobile elements La and Th are more abundant in felsic than in basic rocks while Sc and Co are more concentrated in basic rocks than in felsic rocks (Taylor and McLennan, 1985; Wronkiewicz and Condie, 1987). Scandium and Th are transferred quantitatively from source to sediments and consequently; Th/Sc ratios reflect bulk source compositions (Taylor and McLennan, 1985; McLennan and Taylor, 1991). Furthermore, the variations in these ratios reflect magmatic differentiation (Campos Alvarez and Roser, 2007). Similarly, REE, Th, Sc and the high-field strength elements are especially useful tools for identifying the provenance (Taylor and McLennan, 1985; McLennan and Taylor, 1991). With regard to Zr, it is mostly concentrated in zircons accumulated during sedimentation while fewer resistant phases are preferentially destroyed (Campos Alvarez and Roser, 2007). In this approach, the selected trace elements in stream sediment samples have been employed to provide evidence for their provenance, and sedimentary sorting and recycling. Accordingly, the plotting diagrams of Co/Th versus La/Sc, Th/Co versus Zr/Co, and Th/Sc versus Zr/Sc, have been applied. As well as, La-Th-Sc triangle plot after Cullers (1994) has been used.

5.4. Geochemical maps

The constructions of geochemical maps are more important to perform goals of the present study; they are regarded as effective tools for qualitative and quantitative estimation, and interpretation for the economic and environmental evaluation of the stream sediments in the drainage basin.

5.4.1. Determination of geochemical background and threshold values

In order to draw the geochemical maps and reach more suitable interpretation of the generated geochemical pattern, it is a real need to determine threshold value to discriminate between the background value and the anomaly. Based on the preliminary investigation of the statistical distributions, all chemical elements were possessed non-normal distribution. The median is accepted as the local background value because it is a robust measure of central tendency for data sets with extreme values and not subjected much to the influence of outliers (Ohta et al., 2005; Martínez et al., 2007). Consequently, the median absolute deviation method that has been widely used in recent studies (Reimann et al., 2005) will be effective in the present study. The determination of threshold can be estimated applying the following formula:

$$Threshold = median + 2\ MAD \quad (4)$$

where MAD is the median absolute deviation, a measure of statistical

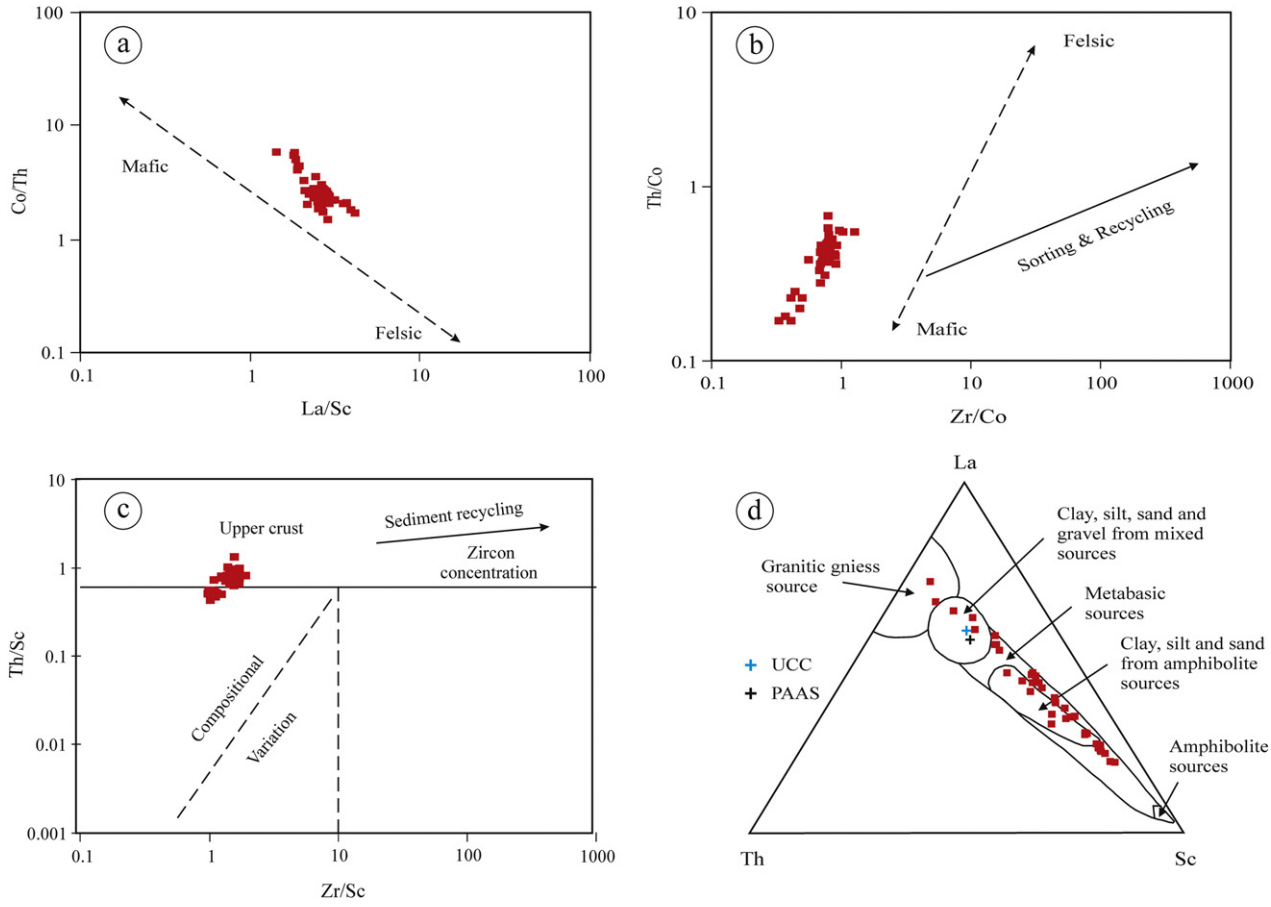

Fig. 3. Sedimentary sorting and provenance discrimination diagrams for the stream sediment data of the Wadi El Quleib area: (a) Co/Th vs. La/Sc and (b) Th/Co vs. Zr/Co. The dashed line represents compositional variation, and the solid line represents sedimentary effects from sorting and recycling. (Taylor and McLennan, 1985 and McLennan and Taylor, 1991), (c) Th/Sc versus Zr/Sc showing reworking and upper crust inputs (after McLennan et al., 1993), and (d) La-Th-Sc ternary plot (Cullers, 1994) compared with Post-Archean Average Shale and Upper Continental Crust (after Taylor and McLennan, 1985).

dispersion, and a robust measure of the variability of a univariate sample of quantitative data. It can be estimated using this equation:

$$MAD = \text{median}\ |X_i - \text{median}\ (X_i)| \quad (5)$$

where X_i is the element concentration.

5.4.2. Single- and multi-element mapping methods

The single element mapping method has been performed for producing geochemical dot maps of the individual elements of interest existed in the stream sediment sampling stations. The size of the dots is proportional to concentrations and defined by median and median plus twice MAD. The threshold values are calculated based on the Eqs. (4) and (5).

Concerning the multi-elements mapping method, Beus and Grigorian (1977) mentioned that geochemical halos around the ore body can be defined better by the combination of two or more pathfinder elements. The multi-element halos are less influenced by the effect of random error and exhibit a closer relationship to structural geological features associated with a mineralization, and thereby the reliability of the interpretation of the halos is increased (Reis et al., 2001). For that reason, multi-element mapping can be constructed according to the following equation.

$$H_{x+z} = (X_1/X_0 + Y_1/Y_0); (X_2/X_0 + Y_2/Y_0); \ldots\ldots\ldots; (X_n/X_0 + Y_n/Y_0) \quad (6)$$

where $X_1, X_2, \ldots, X_N$ are concentrations of X in samples 1, 2, …, N; $Y_1, Y_2, \ldots, Y_N$ are concentrations of Y in samples 1, 2, …, N; and X_0 and Y_0 are background values of X and Y data population (elements). In the same way, the multi-element mapping method was applied for generating geochemical dot maps of the interested combined elements in the sampling stations using the previously criterion as for single-element population. Likewise, the threshold values for the new multi-element data population can be estimated applying the fourth and fifth equations that are used for uni-element populations. The application of median and median plus twice MAD values for multi-element data were also plotted as dot geochemical maps to define their anomalies.

5.5. Potential ecological risk assessment methods

The quantitative and qualitative evaluations of stream sediments can be completed using the ecological risks that were caused by the potential heavy metal(loid)s pollution. Where, the assessments of ecological risk are being susceptible to the dangers of hazardous waste sites, which pose a threat to human health and the environment (Hakånson, 1980). The author has been applied contamination factors, contamination degrees and potential ecological risk indices for the environmental assessment of the examined sediment materials from the Wadi El Quleib area.

5.5.1. The method of contamination level assessment

It can be achieved by the quantification of the contamination factor (C_f^i) and the contamination degree (C_d) after Hakånson (1980). First,

Table 3
Spearman–Rho correlation coefficient matrix of centered log ratio transformed data of chemical elements distributed in the stream sediment sampling stations (N = 40) from the Wadi El Quleib area of the Allaqi region, south Eastern Desert of Egypt.

	Al																			
Al	1.000	Ca																		
Ca	0.467**	1.000	Fe																	
Fe	0.948**	0.489**	1.000	K																
K	0.649**	0.286	0.514**	1.000	Mg															
Mg	0.905**	0.548**	0.899**	0.624**	1.000	Mn														
Mn	0.866**	0.508**	0.876**	0.691**	0.918**	1.000	Na													
Na	−0.699**	−0.447**	−0.639**	−0.548**	−0.605**	−0.603**	1.000	P												
P	0.881**	0.561**	0.876**	0.507**	0.791**	0.773**	−0.536**	1.000	Ti											
Ti	0.555**	0.431**	0.653**	0.269	0.652**	0.707**	−0.184	0.578**	1.000	Ag										
Ag	0.156	0.074	0.082	0.307	0.148	0.243	−0.236	0.170	0.145	1.000	As									
As	0.385*	0.157	0.417**	0.481**	0.520**	0.552**	−0.448**	0.239	0.173	0.181	1.000	Au								
Au	−0.186	−0.040	−0.154	0.013	−0.167	−0.080	0.105	−0.155	−0.257	−0.047	0.242	1.000	B							
B	0.639**	0.318*	0.546**	0.449**	0.444**	0.459**	−0.423**	0.688**	0.230	0.240	0.075	−0.017	1.000	Ba						
Ba	0.775**	0.582**	0.708**	0.865**	0.793**	0.831**	−0.581**	0.730**	0.477**	0.254	0.466**	0.046	0.532**	1.000	Be					
Be	0.704**	0.433**	0.629**	0.609**	0.562**	0.571**	−0.587**	0.726**	0.243	0.106	0.270	−0.114	0.613**	0.648**	1.000	Bi				
Bi	0.201	−0.044	0.204	0.406**	0.097	0.189	−0.186	0.255	0.031	−0.006	0.135	−0.059	0.232	0.344*	0.383*	1.000	Cd			
Cd	0.671**	0.508**	0.634**	0.495**	0.607**	0.642**	−0.617**	0.680**	0.377*	0.089	0.229	0.005	0.475**	0.715**	0.575**	0.250	1.000	Ce		
Ce	0.474**	0.160	0.424**	0.751**	0.384*	0.505**	−0.370*	0.469**	0.133	0.127	0.307	−0.018	0.429**	0.630**	0.610**	0.513**	0.310	1.000	Co	
Co	0.896**	0.573**	0.950**	0.458**	0.939**	0.873**	−0.618**	0.820**	0.679**	0.076	0.504**	−0.184	0.460**	0.682**	0.565**	0.084	0.610**	0.317*	1.000	Cr
Cr	0.704**	0.433**	0.706**	0.531**	0.871**	0.818**	−0.563**	0.561**	0.513**	0.059	0.681**	−0.036	0.251	0.648**	0.357*	−0.079	0.495**	0.296	0.803**	1.000
Cs	0.748**	0.410**	0.629**	0.949**	0.693**	0.744**	−0.660**	0.643**	0.319*	0.337*	0.428**	−0.020	0.520**	0.869**	0.715**	0.387*	0.584**	0.720**	0.563**	0.548**
Cu	0.859**	0.459**	0.920**	0.466**	0.940**	0.878**	−0.549**	0.745**	0.709**	0.039	0.460**	−0.232	0.354*	0.649**	0.462**	0.126	0.544**	0.302	0.935**	0.814**
Ga	0.970**	0.445**	0.897**	0.746**	0.867**	0.860**	−0.661**	0.860**	0.532**	0.218	0.350*	−0.176	0.637**	0.825**	0.718**	0.260	0.685**	0.572**	0.825**	0.653**
Hf	0.526**	0.189	0.422**	0.574**	0.280	0.408**	−0.352*	0.540**	0.172	0.212	−0.003	0.026	0.641**	0.520**	0.519**	0.364*	0.427**	0.656**	0.277	0.161
Hg	0.123	0.264	0.080	−0.027	−0.016	−0.045	−0.328*	0.111	−0.181	0.101	−0.086	0.066	0.152	0.085	0.155	−0.012	0.196	−0.111	0.055	−0.066
La	0.346*	0.034	0.277	0.727**	0.275	0.396*	−0.270	0.315*	0.034	0.075	0.287	−0.023	0.331*	0.557**	0.503**	0.573**	0.234	0.965**	0.184	0.213
Li	0.873**	0.443**	0.776**	0.897**	0.829**	0.837**	−0.709**	0.728**	0.440**	0.223	0.449**	−0.077	0.556**	0.895**	0.690**	0.388*	0.635**	0.666**	0.723**	0.663**
Mo	0.638**	0.300	0.679**	0.637**	0.696**	0.724**	−0.492**	0.571**	0.476**	0.051	0.538**	−0.136	0.434**	0.651**	0.514**	0.442**	0.393*	0.642**	0.679**	0.611**
Nb	−0.524**	−0.231	−0.486**	−0.255	−0.535**	−0.372*	0.382*	−0.389*	−0.146	−0.069	−0.244	0.246	−0.352*	−0.257	−0.392*	0.008	−0.289	−0.098	−0.528**	−0.428**
Ni	0.641**	0.318*	0.629**	0.535**	0.812**	0.759**	−0.537**	0.500**	0.398*	0.103	0.692**	−0.051	0.207	0.609**	0.324*	−0.119	0.500**	0.307	0.729**	0.951**
Pb	0.723**	0.365*	0.640**	0.944**	0.691**	0.749**	−0.660**	0.620**	0.324*	0.271	0.492**	0.009	0.497**	0.862**	0.687**	0.459**	0.517**	0.803**	0.579**	0.571**
Rb	0.632**	0.312	0.493**	0.984**	0.602**	0.660**	−0.548**	0.503**	0.224	0.284	0.436**	0.042	0.441**	0.840**	0.620**	0.378*	0.483**	0.725**	0.438**	0.505**
Sb	0.332*	0.462**	0.361*	0.298	0.397*	0.348*	−0.385*	0.381*	0.242	0.120	0.307	0.158	0.231	0.490**	0.465**	0.307	0.501**	0.170	0.401*	0.300
Sc	0.877**	0.448**	0.837**	0.584**	0.871**	0.868**	−0.526**	0.750**	0.656**	0.149	0.372*	−0.270	0.418**	0.691**	0.475**	−0.003	0.585**	0.391*	0.856**	0.784**
Sn	0.403**	0.071	0.310	0.556**	0.236	0.359*	−0.234	0.445**	0.089	0.241	0.121	−0.083	0.415**	0.436**	0.576**	0.384*	0.269	0.781**	0.202	0.110
Sr	0.641**	0.755**	0.639**	0.198	0.509**	0.462**	−0.620**	0.717**	0.330*	0.012	0.113	−0.152	0.541**	0.459**	0.604**	−0.012	0.565**	0.223	0.642**	0.350*
Th	0.217	−0.262	0.123	0.547**	0.067	0.194	−0.087	0.214	−0.022	0.200	0.135	0.014	0.336*	0.338*	0.309	0.441**	0.136	0.759**	0.021	0.008
Tl	0.566**	0.242	0.447**	0.913**	0.574**	0.627**	−0.501**	0.414**	0.168	0.312*	0.437**	0.057	0.419**	0.776**	0.549**	0.395*	0.369*	0.677**	0.407**	0.459**
U	0.005	−0.334*	−0.063	0.295	−0.118	0.033	0.010	0.077	−0.129	0.234	0.050	0.012	0.158	0.145	0.118	0.284	0.194	0.520**	−0.127	−0.075
V	0.867**	0.484**	0.949**	0.383*	0.812**	0.798**	−0.502**	0.860**	0.679**	0.073	0.367*	−0.048	0.555**	0.607**	0.559**	0.178	0.573**	0.338*	0.901**	0.632**
Y	0.505**	−0.010	0.473**	0.572**	0.413**	0.585**	−0.165	0.475**	0.429**	0.192	0.174	−0.133	0.250	0.483**	0.401*	0.127	0.282	0.702**	0.353*	0.365*
Zn	0.964**	0.440**	0.930**	0.676**	0.856**	0.873**	−0.636**	0.896**	0.603**	0.196	0.385*	−0.127	0.671**	0.792**	0.721**	0.298	0.684**	0.531**	0.856**	0.622**
Zr	0.440**	0.276	0.304	0.694**	0.253	0.366*	−0.291	0.447**	0.096	0.130	0.122	0.145	0.556**	0.585**	0.625**	0.272	0.369*	0.705**	0.216	0.174

N = number of sampling stations; *. = correlation is significant at the 0.05 level (2-tailed); **. = correlation is significant at the 0.01 level (2-tailed).

Table 3 *(continued)*

Al																											
Ca																											
Fe																											
K																											
Mg																											
Mn																											
Na																											
P																											
Ti																											
Ag																											
As																											
Au																											
B																											
Ba																											
Be																											
Bi																											
Cd																											
Ce																											
Co																											
Cr	Cs																										
Cs	1.000	Cu																									
Cu	0.531**	1.000	Ga																								
Ga	0.832**	0.788**	1.000	Hf																							
Hf	0.596**	0.189	0.623**	1.000	Hg																						
Hg	0.016	−0.044	0.080	0.118	1.000	La																					
La	0.656**	0.192	0.463**	0.590**	−0.158	1.000	Li																				
Li	0.933**	0.731**	0.909**	0.561**	0.036	0.599**	1.000	Mo																			
Mo	0.650**	0.660**	0.652**	0.372*	−0.137	0.589**	0.721**	1.000	Nb																		
Nb	−0.374*	−0.494**	−0.485**	−0.055	0.051	−0.010	−0.395*	−0.398*	1.000	Ni																	
Ni	0.536**	0.736**	0.613**	0.121	−0.069	0.244	0.609**	0.584**	−0.455**	1.000	Pb																
Pb	0.950**	0.574**	0.785**	0.575**	0.002	0.741**	0.926**	0.718**	−0.327*	0.545**	1.000	Rb															
Rb	0.952**	0.440**	0.727**	0.559**	0.018	0.693**	0.888**	0.602**	−0.259	0.509**	0.940**	1.000	Sb														
Sb	0.342*	0.335*	0.299	0.128	0.158	0.092	0.391*	0.367*	−0.100	0.230	0.346*	0.287	1.000	Sc													
Sc	0.659**	0.825**	0.873**	0.450**	−0.062	0.296	0.756**	0.584**	−0.450**	0.739**	0.604**	0.559**	0.148	1.000	Sn												
Sn	0.569**	0.158	0.497**	0.641**	0.036	0.756**	0.495**	0.421**	−0.122	0.155	0.569**	0.556**	0.004	0.330*	1.000	Sr											
Sr	0.368*	0.464**	0.587**	0.379*	0.447**	0.065	0.440**	0.317*	−0.352*	0.287	0.316*	0.219	0.340*	0.510**	0.255	1.000	Th										
Th	0.437**	0.005	0.322*	0.632**	−0.123	0.784**	0.394*	0.346*	0.038	0.066	0.537**	0.500**	−0.030	0.156	0.645**	−0.093	1.000	Tl									
Tl	0.870**	0.427**	0.641**	0.433**	−0.037	0.662**	0.817**	0.563**	−0.289	0.482**	0.884**	0.920**	0.268	0.484**	0.430**	0.124	0.481**	1.000	U								
U	0.200	−0.160	0.107	0.496**	0.027	0.558**	0.128	0.158	0.130	0.063	0.244	0.253	−0.021	0.033	0.579**	−0.120	0.831**	0.207	1.000	V							
V	0.509**	0.846**	0.814**	0.432**	0.060	0.187	0.652**	0.623**	−0.424**	0.525**	0.514**	0.368*	0.347*	0.777**	0.263	0.633**	0.067	0.310	−0.102	1.000	Y						
Y	0.568**	0.380*	0.615**	0.585**	−0.213	0.646**	0.532**	0.472**	−0.046	0.387*	0.555**	0.542**	−0.086	0.613**	0.674**	0.118	0.596**	0.422**	0.489**	0.442**	1.000	Zn					
Zn	0.765**	0.821**	0.955**	0.554**	0.055	0.415**	0.871**	0.672**	−0.442**	0.559**	0.744**	0.649**	0.352*	0.830**	0.460**	0.607**	0.291	0.569**	0.060	0.867**	0.554**	1.000	Zr				
Zr	0.680**	0.113	0.514**	0.730**	0.086	0.654**	0.580**	0.279	−0.014	0.123	0.661**	0.719**	0.158	0.369*	0.671**	0.323*	0.573**	0.592**	0.349*	0.305	0.524**	0.484**	1.000				

contamination factor (C_f^i) has been calculated as the ratio between the heavy metal(loid)s' concentrations in the sediments and the corresponding background values as established by Guillén et al. (2011):

$$C_f^i = C_{heavy\ metal}/C_{background} \quad (7)$$

The mentioned relationship shows the range of naturally-occurring concentrations of these metal(loid)s; their natural variability is considered for identifying and assessing the intensity of anthropogenic metals in the sediment substances.

Four classes of contamination factors could be characterized as suggested by Hakånson (1980): $C_f^i < 1$, low contamination; $1 \le C_f^i < 3$, moderate contamination; $3 \le C_f^i < 6$, considerable contamination; $C_f^i \ge 6$, very high contamination.

Second, contamination degree (C_d) can be estimated as the summation of contamination factors (C_f^i) of considerable heavy metal(loid)s as follows:

$$C_d = \sum_{i=1}^{m} C_f^i \quad (8)$$

where m refers to the count of the heavy metal(loid)s' species. Caeiro et al. (2005) and Pekey et al. (2004) proposed four levels of contamination degrees: $C_d < m$, low degree of contamination; $m \le C_d < 2$ m, moderate degree of contamination; $2\ m \le C_d < 4$ m, considerable degree of contamination; $4\ m \le C_d$, very high degree of contamination.

5.5.2. The method of potential ecological risk assessment

Hakånson (1980) suggested the quantitative method to determine the potential ecological risk generated from excess of heavy metal(loid)s' concentrations. In analogy with the previous calculations of the contamination factor and the degree of contamination, the potential ecological risk factor (E(i)) and potential ecological risk index (RI) have been computed. This method has been widely applied to assess the pollution of sediment and soil (Li et al., 2011), and is more comprehensive for estimating potential ecological risk assessment because it considers the diverse potential toxic-response factors for different heavy metal(loid)s' concentrations.

First, the potential ecological risk factor can be calculated as follows:

$$E(i) = T_i \times (C_i/C_o) \quad (9)$$

where E(i) is the potential ecological risk factor for a given pollutant (i); T_i refers to the "toxic-response" factor for a given pollutant (i) as calculated by Hakånson (1980) and Xu et al. (2008), for instance, Hg = 40, Cd = 30, As = 10, Co = Ni = Cu = Pb = 5, Cr = V = 2, Ti = Mn = Zn = 1; C_i represents the heavy metal(loid) content in the topsoil; C_o denotes the regional background value of heavy metal(loid) in the topsoil. Hakånson (1980) used the following terminology to describe the risk factor: $E(i) < 40$, low potential ecological risk; $40 \le E(i) < 80$, moderate potential ecological risk; $80 \le E(i) < 160$, considerable potential ecological risk; $160 \le E(i) < 320$, high-potential ecological risk; $E(i) \ge 320$, the very high-potential ecological risk.

Second, the potential ecological risk index (RI) for an area can also be defined according to Hakånson (1980) as follows:

$$RI = \sum_{i=1}^{n} E(i) \quad (10)$$

where $\Sigma E(i)$ is the sum of the individual potential risks' factors. The RI is divided into four levels: $RI < 150$, refers low ecological risk; $150 \le RI < 300$, represents moderate ecological risk; $300 \le RI < 600$, expresses as considerable ecological risk; $RI \ge 600$, denotes very high ecological risk. Due to the median values for stream sediments were not computed by Egyptian Government organizations, the author could apply the average concentrations of the elements in the upper continental crust of the earth "UCC" as background value (Table 1) for computing the Eqs. (6), (7), and (9).

In the present study, all data processing, calculations, graphic representation and visualization (mapping) have been achieved by applying the following software: Origin Pro 8 (Origin Lab Corporation, 2008); SPSS Statistics 17 (SPSS Inc., 2007); Corel Draw 12 (Corel Corporation, 2003); and Surfer 8 (Golden Software Inc., 2002).

6. Results and discussions

6.1. Descriptive statistics

The calculated statistical parameters generated from the analyses' the stream sediment data were listed in Table 1, which shows remarkable deviations between means and medians, and standard deviations and mean absolute deviations for the most considered elements. Table 1 display that Ag possesses concentration range (20 to 89 ppb) and mean value (33.9 ppb) greater than the values of range (0.1 to 7 ppb) and average value (0.89 ppb) of Au. The lack of Au content is probably caused by traditional exploitation and extraction methods of Au using streambed sediments during the past as observed by the previously mentioned aspects of old mining works within the area. Despite most analyzed elements have low standard deviation and small variance values, the remaining elements have high variance, such as Mn (9280), Ba (546.5), Cr (239), Ag (187.9), Ni (112.3), V (108.9), Zn (71.02), Sr (53.39), Ce (40.98), and Hg (36.92). The variation in concentrations' ranges of the determined elements might be generated by the action of physical and chemical weathering on the drainage basin beside the monitored anthropogenic activities.

Skewness values have positive values ranging from 0.42 (for Cd) to 6.2 (for Na) and deviate away from zero values, and kurtosis values change from −0.48 (for B) to 38.95 (for Na) as listed in Table 1. Their values are due to the effects of outliers, mixture of populations, analytical precision or detection limits of the data set (Zhang et al., 2005). The calculated Shapiro-Wilk (S–W) test reveals that all analyzed elements (except for Zr, Nb and Cd) could not pass the normality test (p-values < 0.05), indicating that they did not follow the normal distribution and thus, the null hypothesis is rejected. Despite Zr, Nb and Cd have skewness deviated from zero values, they are also deviated from the normality (Table 1). Under these circumstances, it is a real need to use the logarithmic transformations for all element concentrations in order to decrease the effect of outliers and extremes, the deviation from normality, and avoid misleading and seriously biased the results of further statistical treatments. Center-log ratio transformation (clr) was chosen not only for improving the statistical distribution toward normality but also for treating the closure problem in the multivariate statistical analysis of compositional data sets and all components symmetrically, and enabling an easier interpretation of single clr variables in the sense of the original compositional parts (Filzmoser et al., 2009; Reimann et al., 2012).

6.2. Weathering

The plotting of the CIA values is observed in Al_2O_3–($CaO^* + Na_2O$)–K_2O diagram of Nesbitt and Young (1982, 1984, 1989), which displays the weathering trend and probable parent source rocks (Fig. 2). The calculated CIA values vary from 36.13 to 62.81 with an average of 48.75 (Table 2); this demonstrates that the degree of chemical weathering or alteration intensity was ranging from low to moderate at the source area. According to Fig. 2, a portion of analyzed samples existed below the plagioclase – K-feldspar tied line (CIA < 50) refer to be very poor weathering conditions or albitic-rich sources with less K mobility (Hossain et al., 2014). Another portion of samples was plotted above the plagioclase – K-feldspar tied line and below average post-Archean Australian shale "PAAS", implying that these samples are not enriched in Al_2O_3 and tend toward moderate weathering. The low CIA values

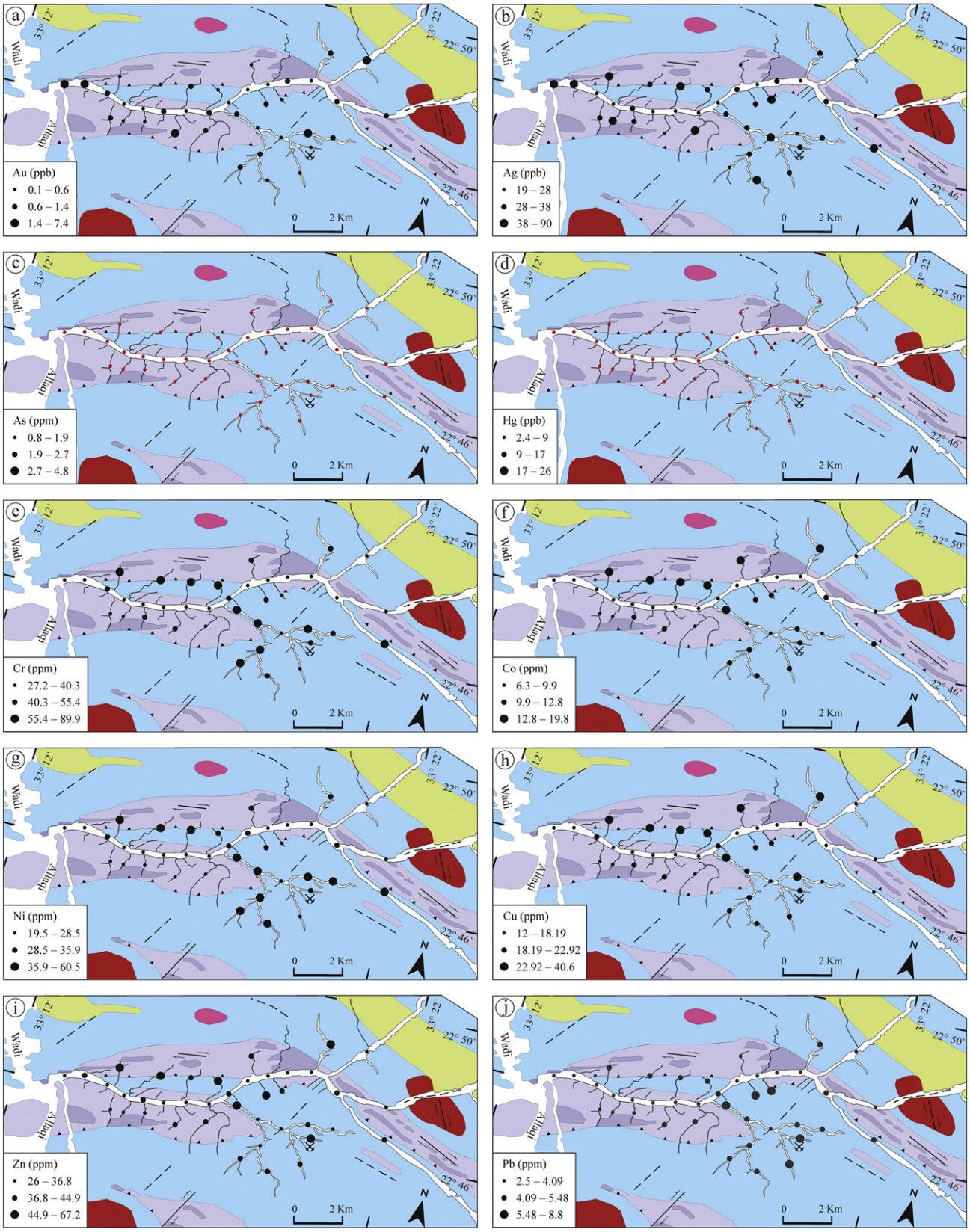

Fig. 4. Geochemical dot maps of (a) Au, (b) Ag, (c) As, (d) Hg, (e) Cr, (f) Co, (g) Ni, (h) Cu, (i) Zn, and (j) Pb concentrations distributed in the stream sediments in relation to lithologic units of the Wadi El Quleib area. Minimum values are median; moderate values are median + 2MAD; high values are anomalies (the probable mineralized sites). For lithological units look at Fig. 1.

suggest less intense weathering produced sand-sized sediments, while the moderate CIA values may be implied longer residence times, and consequently, more intense weathering generated very fine-grained silt and mud in the samples (Bhuiyan et al., 2011). For this reason, the degrees of weathering are fairly different throughout the stream sediments, indicating non steady-state weathering conditions in the source

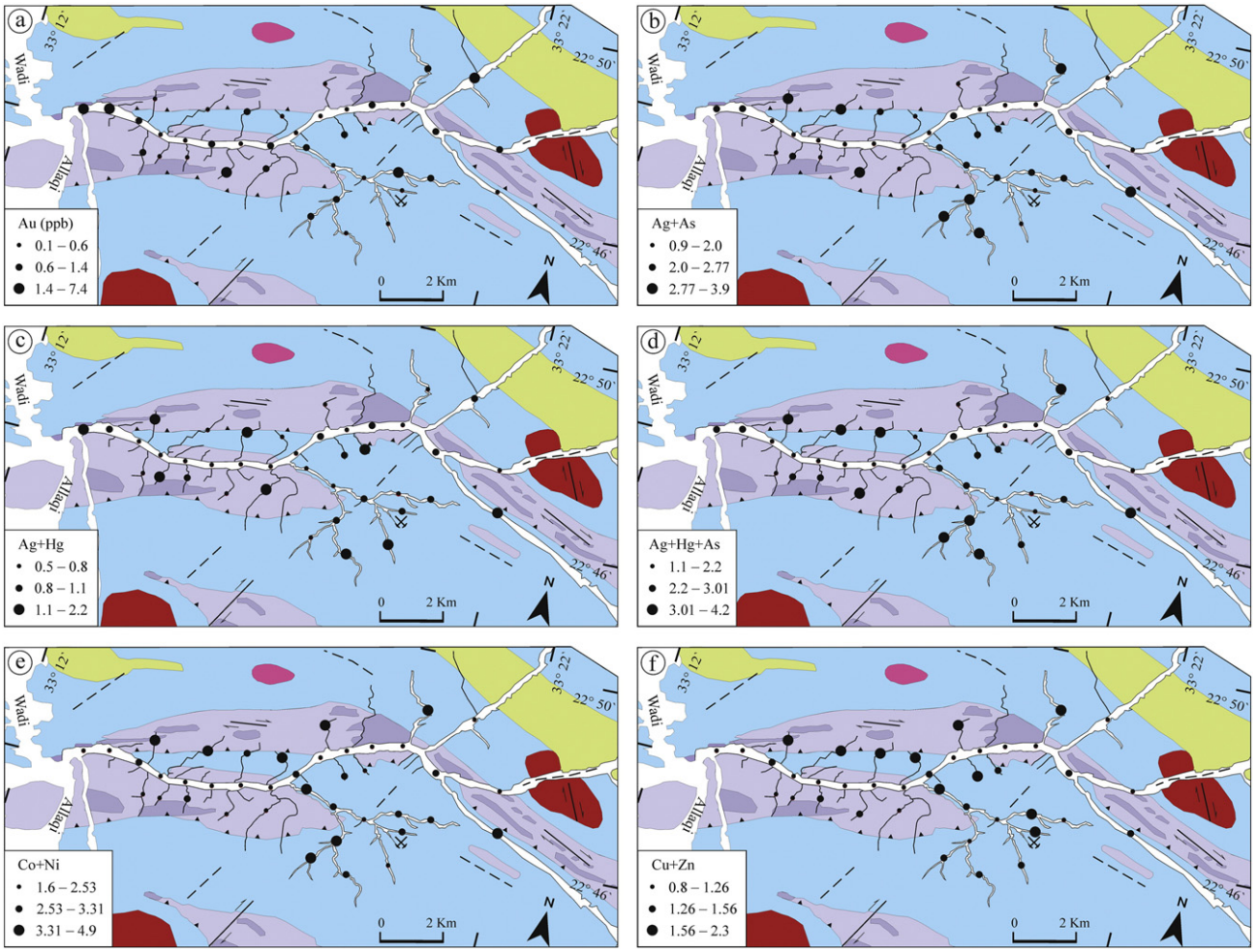

Fig. 5. Geochemical dot maps of (a) Au and multi-elements of (b) Ag + As, (c) Ag + Hg, (d) Ag + Hg + As, (e) Co + Ni, and (f) Cu + Zn distributed in the stream sediments in relation to lithologic units of the Wadi El Quleib area. Minimum values are median; moderate values are median + 2MAD; high values are anomalies (the probable mineralized sites). For lithological units look at Fig. 1.

area (Nesbitt et al., 1997); this is probably due to increases in the intensity of tectonic activity throughout some periods of time at least, which permits rapid erosion of source rocks (Hossain et al., 2014).

The calculated CIW values in the stream sediments (Table 2) vary from 37.88 to 68.20 (average 51.88), and Sr contents range between 27.8 and 56.7 (average 37.76) as seen in Table 1. These values are lower than corresponding values of most post Archean shales that possess CIW range between 80 and 95, and Sr content varies from 75 to 200 ppm (Condie, 1993). The calculated ICV values in all samples are high and ranging from 1.68 to 2.54 with average 2.15 (Table 2); such values are typical of minerals like plagioclase, K-feldspar, amphiboles, and pyroxenes (Cox et al., 1995).

Table 4
Summarized statistics of the generated multi-elements data showing their geochemical background and threshold values in the stream sediment sampling stations (N = 40) from the Wadi El Quleib area of the Allaqi region, south Eastern Desert of Egypt.

Element(s)	Minimum	Mean	Maximum	Background	MAD	Threshold
Ag + As	1.00	2.17	3.78	2.03	0.37	2.77
Ag + Hg	0.55	0.90	2.17	0.81	0.15	1.10
Ag + Hg + As	1.20	2.39	4.17	2.24	0.39	3.01
Co + Ni	1.62	2.74	4.81	2.53	0.39	3.31
Cu + Zn	0.87	1.36	2.22	1.26	0.15	1.56

N: number of sampling stations; MAD: median absolute deviation; Background: median; Threshold: median plus twice MAD.

As you can see, the results of CIA, CIW and ICV values in the sediment materials are not typical of shales, indicating less intense source area weathering, and probably reflecting the existence of clay minerals associated with detrital minerals and detritus clastics of igneous and metamorphic rocks.

These are supported by the low K_2O/Al_2O_3 ratios varied from 0.05 to 0.17 with mean value of 0.11(Table 2), which emphasizes the importance of the clay fraction in determining the bulk compositions of the sediment materials (Campos Alvarez and Roser, 2007). Overall, CIA, CIW and ICV values are indicative of their effectiveness to image the weathering history that was not seemed to be simple. Another possible explanation suggests that study area might be affected by more than one weathering cycle.

6.3. Provenance

The diagram of Co/Th against La/Sc, (Fig. 3a) exhibits that the stream sediments are a mixture of felsic and mafic rock end members; they are clustered toward mafic rock's end member, revealing their mafic nature. The mafic nature of the stream sediment materials is confirmed by their high contents of Co and Sc, and the strong and very strong positive correlation of Sc with Ti (rs = 0.656), Ni (rs = 0.739), V (rs = 0.777), Cr (rs = 0.784), and Co (rs = 0.856) (Table 3). Similarly, the very strong positive correlation between Fe and Mg (rs = 0.899) in the stream sediments also implies the dominance of mafic rocks (Wu et al., 2011). Regarding to Fig. 3b showed the plotting of Th/Co versus Zr/Co, the stream

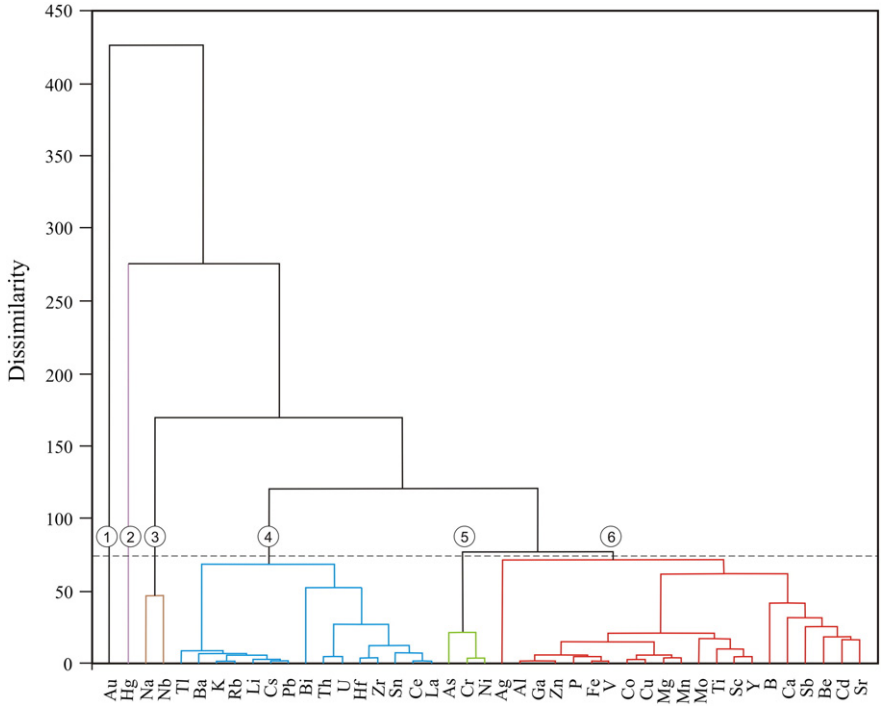

Fig. 6. Hierarchical clustering dendrogram based on centered log-ratio transformation for the analyzed elements distributed in the stream sediments of the Wadi El Quleib area.

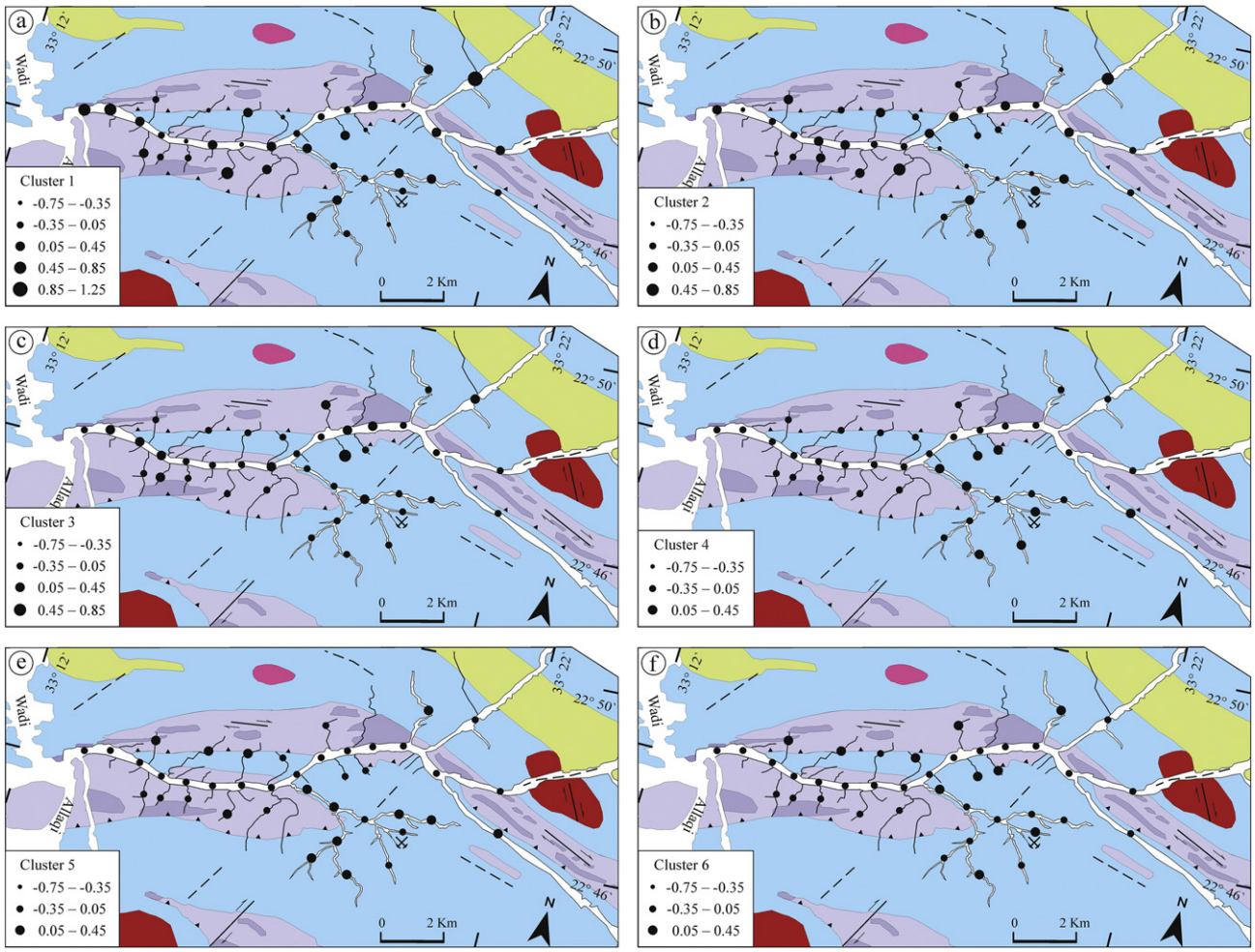

Fig. 7. Geochemical dot maps of the six clusters deduced from cluster analysis and dispersed in the stream sediments of the Wadi El Quleib area. For lithological units look at Fig. 1.

sediment materials did not follow the sedimentary sorting and recycling trend, which lead to an enrichment of the heavy minerals (mainly for zircon). Besides, they have low Zr/Co and Th/Co values and high concentration of Co, confirming the mafic nature of the stream sediment samples in the study area.

Likewise, Fig. 3c reveals that the sediment samples have a slightly increase in Th/Sc ratios and a substantial decrease in Zr/Sc ratios, implying the deviation of samples away from the direction of sediment recycling and zircon concentration too. The obtained results are in accordance with Nesbitt et al. (1996) who mentioned that the decreased Zr/Sc ratios did not indicate sedimentary sorting and mild recycling. In addition, together with Taylor and McLennan (1985) who suggested that low Zr/Sc ratio can be used as a tracer for zircon or heavy mineral concentration. Therefore, zircon or other heavy minerals were not concentrated in the drainage basin because there is no sedimentary provenance, enrichments related to sedimentary transport and no mild effect of hydraulic sorting.

The La-Th-Sc ternary diagram shows that the stream sediment materials are predominantly existed within the field of metabasic source, and the field of clay, silt and sand derived from amphibolite source (Fig. 3d). The basic materials of the stream sediments were derived from ultramafics and their derivatives, and volcanogenic metasediments. In contrary, few amounts of sediment samples fall in both fields of clay, silt, sand and gravel from mixed source and granitic gneiss source. The minor contribution of mixed sources is close to the values of UCC, and PAAS, suggesting that La, Th, and Sc in the corresponding sediments' sites have remained immobile regardless of the active weathering act in the area evidenced by the sediments' formation. Generally, the drainage basin of the study area was charged with stream sediments containing clastic components principally derived from the metamorphosed mafic and ultramafic rocks rather than mixed and felsic rocks of Egyptian basement complex.

6.4. Geochemical maps

The single element dots geochemical maps for Cr and the most probable elements associated with Au (like, Co, Ni, Cu, Zn, Ag, Hg, Pb and As) in the Wadi El Quleib catchment area have been prepared (Fig. 4a–j). The geochemical pattern of Au shows that the median + 2MAD values are noticed in the most sites throughout the study area beside five anomalies. The generated anomalies are observed in the entrance of the Wadi El Quleib, and tributaries of drainage sub-basin and the metamorphosed ultramafics and their derivatives (Fig. 4a). As it was previously stated, the limited Au anomalous sites within the drainage basin might be due to the disturbances caused by former ore and mining activities performed over the past. Another probable illustration suggesting that the Au may be concentrated at deeper levels within streambed sediments. The presence of Au anomalous site associated with Hg anomaly in the northeastern part, along tributary trending NE-SW direction, will require further investigation. On contrary, the geochemical pattern of Ag exhibiting the median, median plus twice MAD, and anomaly values are more dispersed compared to Au pattern. Moreover, Ag-anomalous sites are not coincided with those of Au except two Ag-anomalies at the mouth of the Wadi El Quleib (Fig. 4b). This is suggestive of the mobility, behavior and concentration of both Au and Ag in secondary environment are different, and their differences are proved by the negative correlation between both elements (Table 3). Furthermore, Ag anomalous sites are also observed along tributaries of the metamorphosed ultramafic and related rocks, volcanogenic metasediments and their thrust contact.

Despite the different distribution patterns of Ag and As, As anomalies are monitored along the tributaries inside metamorphosed ultramafic and their derivatives, volcanogenic metasediments, and those crossed the tectonic contact (Fig. 4c). Concerning the geochemical pattern of Hg, the anomalous sampling stations are commonly restricted to the tributaries of metamorphosed ultramafic and related rocks and the drainage sub-basin (Fig. 4d).

It can be noticed that the anomalous geochemical patterns of Cr and Ni are similar spatial pattern; they are concentrated along the tributaries crossing the thrust fault and enhanced in the drainage sub-basin (Fig. 4e & g). Cr anomalies might be indicative of Cr-mineralization associated with metamorphosed ultramafic and related rocks. Since the remarkable anomalous values of Ni and As can be seen along tributaries cutting aforementioned contact and enhance in drainage sub-basin involving the previously detected an ancient gold mine, both elements are considered as a more useful element for Ni-bearing minerals. Fig. 4f shows that Co-anomalies mainly appeared along the tributaries run through the mentioned ultramafic and their derivatives. The geochemical patterns of Cu and Zn possess similar anomalous sites; they are predominantly observed along the tributaries cutting the tectonic contact (Fig. 4h & i). In contrast, Pb anomalous sites are defined within and near to the drainage sub-basin (Fig. 4j).

Table 5
Principal component analysis of centered log ratio transformed data of chemical elements distributed in the stream sediment sampling stations (N = 40) from the Wadi El Quleib area of the Allaqi region, south Eastern Desert of Egypt.

Elements	Components			
	PC1	PC2	PC3	PC4
Al	**0.819**	0.445	0.236	0.063
Ca	0.414	0.146	**0.572**	0.142
K	0.188	**0.959**	−0.045	0.106
Mg	**0.889**	0.305	0.009	0.215
Na	0.056	0.112	**−0.511**	**−0.632**
Fe	**0.917**	0.297	0.114	0.045
Mn	**0.815**	0.445	−0.058	0.271
P	**0.852**	0.297	0.158	−0.291
Ti	**0.903**	−0.015	−0.065	−0.083
Ag	0.015	0.099	0.111	0.096
As	0.257	0.243	−0.093	**0.730**
Au	−0.203	−0.005	0.018	0.066
B	0.367	0.467	0.427	−0.272
Ba	0.491	**0.769**	0.126	0.128
Be	0.380	**0.655**	0.431	0.025
Bi	−0.032	0.485	−0.044	−0.121
Cd	**0.530**	0.267	0.481	0.254
Ce	0.188	**0.888**	0.002	−0.069
Co	**0.946**	0.048	0.171	0.206
Cr	**0.736**	0.155	−0.002	**0.572**
Cs	0.309	**0.929**	0.081	0.029
Cu	**0.967**	0.012	0.045	0.117
Ga	**0.720**	**0.621**	0.170	−0.009
Hf	0.193	**0.644**	0.282	−0.278
Hg	−0.097	−0.065	**0.748**	−0.094
La	0.069	**0.912**	−0.082	−0.053
Li	**0.521**	**0.823**	0.066	0.074
Mo	**0.565**	**0.564**	−0.059	0.228
Nb	**−0.539**	−0.061	−0.170	−0.281
Ni	**0.584**	0.152	−0.018	**0.707**
Pb	0.301	**0.918**	0.017	0.129
Rb	0.157	**0.964**	−0.001	0.117
Sb	0.223	0.101	0.289	0.238
Sc	**0.876**	0.308	0.020	0.115
Sn	0.201	**0.719**	0.164	−0.150
Sr	**0.515**	0.044	**0.781**	0.013
Th	−0.053	**0.645**	−0.120	−0.062
Tl	0.050	**0.942**	−0.063	0.176
U	−0.113	0.249	0.026	0.099
V	**0.956**	0.126	0.105	−0.074
Y	0.373	**0.599**	−0.144	0.042
Zn	**0.756**	**0.564**	0.116	−0.016
Zr	0.069	**0.817**	0.286	−0.120
Eigenvalue	20.228	7.073	2.612	2.392
Variability (%)	47.042	16.449	6.074	5.563
Cumulative %	47.042	63.491	69.565	75.128

N: number of sampling stations; Loading values for the PC axis higher than +0.5 and lower than −0.5 are given in bold.

Besides both As and Ni, Co, Cu, Zn, Ag, and Hg must be taken into account due to their known significance for exploring the Au mineralization; their combinations of two or three elements are effective and facilitate for defining the sought Au mineralization in the study area. Lead was excluded because it did not cause significant indication when combined with both Cu and Zn. In this approach, the geochemical dot maps for multi-elements: Ag + As, Ag + Hg, Ag + Hg + As, Co + Ni and Cu + Zn have been constructed (Fig. 5b–f) based on their generated data listed in Table 4. The anomalous sites of combined elements Ag + As, and Ag + Hg + As are similar; they are clearly distributed in the drainage sub-basin, and along tributaries cut both the mentioned contact and the metamorphosed ultramafic and related rocks (Fig. 5b & d). In the same way, the anomalous sites of Ag + Hg are predominantly observed along the tributaries of volcanogenic metasediments and related drainage sub-basin, and the mentioned ultramafic rocks and their contact (Fig. 5c) Although the anomalous patterns of the association of Co + Ni and Cu + Zn are slightly different; they were mainly monitored along tributaries crossing thrust contact and drainage sub-basin (Fig. 5e & f).

Accordingly, the combination of Ag + As, Ag + Hg, and Ag + Hg + As are indicative of Au mineralization and are regarded as useful pathfinders for it. Whereas, Cu + Zn and Co + Ni anomalous patterns are suggestive of Ni-bearing minerals.

In the drainage sub-basin, the anomalous sites of As, Cr, Ni, As + Ag, As + Hg + Ag, and Co + Ni are concordant with NNE-SSW trending faults; then these faults need further investigations. As mentioned before the drainage sub-basin included the previously mentioned gold mine, the examined geochemical maps of single As and Ni, and the aforesaid multi-elements are helpful and significant for geochemical detailed survey and exploration in the study area. It can be concluded that the feeding channels represented by thrust contact, faults and their hidden fracture zones, and lithology (volcanogenic metasediments, metamorphosed ultramafic and their derivatives) could play an important role to feed and control the localization of sought Au mineralization in primary environment, and the related anomalous sites generated in the secondary environments of the study area. Accordingly, the mentioned lithology and tectonic zones are regarded as the preferred hosts for Au mineralization.

6.5. Geochemical signatures

They are helpful to discriminate between different groups of element contents that dispersed into the stream sediment's environment; the generation of geochemical signatures is due to their geochemical affinity and input sources. Six geochemical associations have been distinguished according to R-mode cluster analysis applying Ward's method and Euclidean distance (Fig. 6) and named as follows: cluster 1 includes only Au; cluster 2 contains Hg alone; cluster 3 associates Na, and Nb; cluster 4 consists of Tl, Ba, K, Rb, Li, Cs, Pb, Bi, Th, U, Hf, Zr, Sn, Ce, and La; cluster 5 has As, Cr, and Ni; and cluster 6 composes of Ag, Al, Ga, Zn, P, Fe, V, Co, Cu, Mg, Mn, Mo, Ti, Sc, Y, B, Ca, Sb, Be, Cd and Sr.

The limited sites with high values of cluster 1 (Au) appeared in the catchment basin (Fig. 7a) confirming the disturbance of Au levels in the stream sediments caused by extensively sieving processes of stream sediment materials and recovery processes for gold over the past. Similarly, Hg in cluster 2 could not be grouped with other elements; this verifies the chemical properties, and behavior of Hg and remains elements in secondary environment are dissimilar. The distribution of high values of cluster 2 is supporting the local Hg anomalies scattered throughout the catchment basin (Fig. 7b). Undeniably, Hg is not represented anthropogenic input of former Au recovery processes and mining workings due to its normalized values relative to UCC are less than unity. Therefore, Hg is principally related to geogenic processes, and potentially associated with Au mineralization. Cluster 3 (Na and Nb association) plotted in Fig. 7c showed the moderate values might be related to detritus minerals derived from metamorphosed ultramafic and volcanogenic metasediment units, while the high value is related to the latter lithologic unit. So that, cluster 3 points to the action of weathering processes and the element association are geologically inputs.

Table 6
Summarized statistics of risk assessment obtained by contamination factors (C_f^i), contamination degrees (C_d) and potential ecological risk factors (E(i)), and ecological risk index (RI) for chosen heavy metals and metalloid, illustrating their contamination and risk levels in the stream sediment sampling stations (N = 40) from the Wadi El Quleib area of the Allaqi region, south Eastern Desert of Egypt.

	Minimum	Mean	Maximum	Median	MAD	Contamination and risk level
C_f^i						
Ti	0.28	0.36	0.61	0.33	0.03	Low contamination factor
V	0.52	0.80	1.27	0.76	0.09	Low contamination factor
Cr	0.78	1.33	2.57	1.16	0.22	Moderate contamination factor
Mn	0.43	0.66	1.01	0.61	0.07	Low contamination factor
Co	0.64	1.09	1.96	0.99	0.15	Moderate contamination factor
Ni	0.98	1.65	3.02	1.43	0.19	Moderate contamination factor
Cu	0.48	0.81	1.62	0.73	0.09	Low contamination factor
Zn	0.37	0.55	0.95	0.52	0.06	Low contamination factor
Cd	0.51	0.92	1.53	0.82	0.20	Low contamination factor
Hg	0.05	0.22	0.54	0.20	0.09	Low contamination factor
Pb	0.14	0.22	0.44	0.20	0.03	Low contamination factor
As	0.60	1.49	3.13	1.27	0.27	Moderate contamination factor
C_d	6.15	10.09	16.73	9.56	1.41	Low degree of contamination
E(i)						
Ti	0.28	0.36	0.61	0.33	0.03	Low potential ecological risk
V	1.03	1.60	2.53	1.52	0.18	Low potential ecological risk
Cr	1.56	2.66	5.13	2.30	0.43	Low potential ecological risk
Mn	0.43	0.66	1.01	0.61	0.07	Low potential ecological risk
Co	3.20	5.48	9.80	4.95	0.73	Low potential ecological risk
Ni	4.90	8.27	15.10	7.15	0.93	Low potential ecological risk
Cu	2.42	4.05	8.10	3.64	0.47	Low potential ecological risk
Zn	0.37	0.55	0.95	0.52	0.06	Low potential ecological risk
Cd	15.31	27.55	45.92	24.49	6.12	Low potential ecological risk
Hg	2.20	8.68	21.70	7.80	3.48	Low potential ecological risk
Pb	0.69	1.09	2.18	1.02	0.17	Low potential ecological risk
As	6.00	14.90	31.30	12.70	2.67	Low potential ecological risk
RI	41.27	75.81	110.93	71.01	11.19	Low ecological risk

N: number of sampling stations; MAD: median absolute deviation.

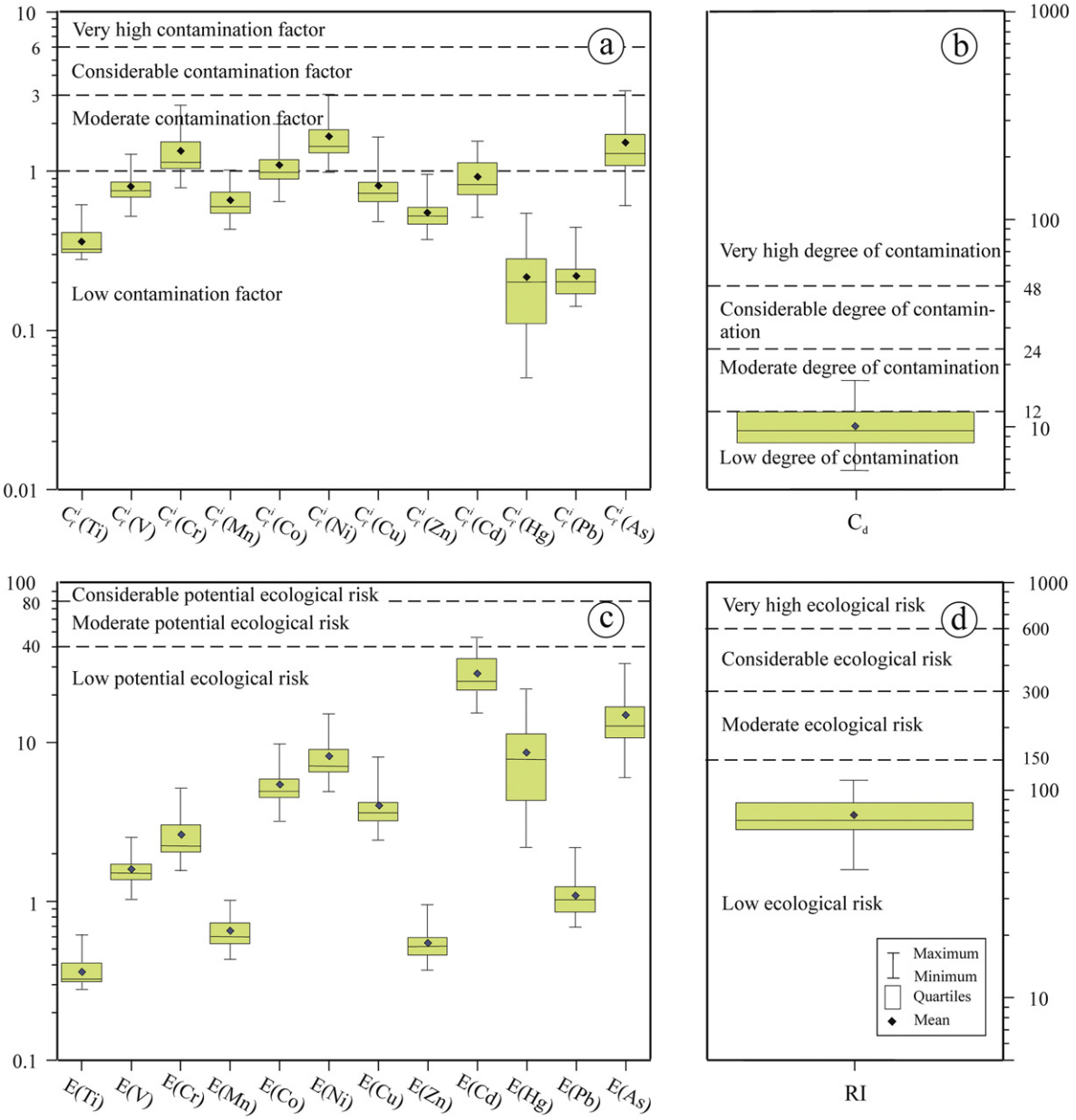

Fig. 8. Box-plot representations for the assessment of the selected heavy metals dispersed in the stream sediments of the Wadi El Quleib area: (a) contamination factors "C_f^i", (b) contamination degrees "C_d", (c) potential ecological risk factors "E(i)", and (d) potential ecological risk indices "RI".

The high values of cluster 4 (Tl, Ba, K, Rb, Li, Cs, Pb, Bi, Th, U, Hf, Zr, Sn, Ce, and La association) appear in the tributaries of volcanogenic metasediments and granitic rock (Fig. 7d), verifying the element association of this factor derived from the mentioned rock units. Because the lithophile elements such as Ba, K, Rb, Li and Cs are indicative of granitic rocks (Pohl and Emmermann, 1991; Zhang and Wang, 2001); Li, Sn, and Pb are typically related to felsic source (Harraz et al., 2012) of volcanogenic metasediments; and Th, U, Hf, Zr, Ce were mainly derived from both felsic sources and granitoid protoliths (Moreno et al., 2006; Kalender and Uçar, 2013). In addition to the latter elements, La and Sn are abundant in host accessory minerals such as zircon, ilmenite, rutile, monazite, apatite, and sphene that influence their levels (Chandrajith et al., 2001). It can be concluded that the elemental association of cluster 4 was also controlled by natural origin.

Cluster 5 (As, Cr and Ni association) is mainly dispersed in the drainage sub-basin of volcanogenic metasediments, which involves an ancient gold mine and the tributaries cutting the thrust fault (Fig. 7e). Therefore, their elevated values refer to the old anthropogenic influences of previously mentioned mining activities and weathering products of the metamorphosed ultramafic rocks and volcanogenic metasediments. Cluster 5 confirmed a presence of disseminated Ni–sulfides and Ni–arsenides, and chromite lenses hosted by thrust contact and metamorphosed ultramafic rocks, respectively. This is supported by the normalized values of As, Cr and Ni against UCC in the streambed sediments exceeds unity. Moreover, the concentrations of both Cr and Ni in serpentines reach 2540 and 143.4 ppm, and in metavolcanic rocks reach 500 and 809 ppm, respectively (obtained from data published by El Afandy et al., 2007). Finally, the outlined high values of cluster 6 (Ag, Al, Ga, Zn, P, Fe, V, Co, Cu, Mg, Mn, Mo, Ti, Sc, Y, B, Ca, Sb, Be, Cd and Sr association) can be noticed along tributaries of volcanogenic metasediments and metamorphosed ultramafic rocks, and near the above-mentioned fault (Fig. 7f); thus, it reflects that detrital grains of the mentioned rocks and their related minerals could play a significant role in the formation of this elemental association. This finding is verified by remarkable very strong positive correlations ($rs \geq 0.8$) of Al with Ga, Zn, P, Fe, V, Co, Cu, Mg, Mn, and Sc; strong positive correlation

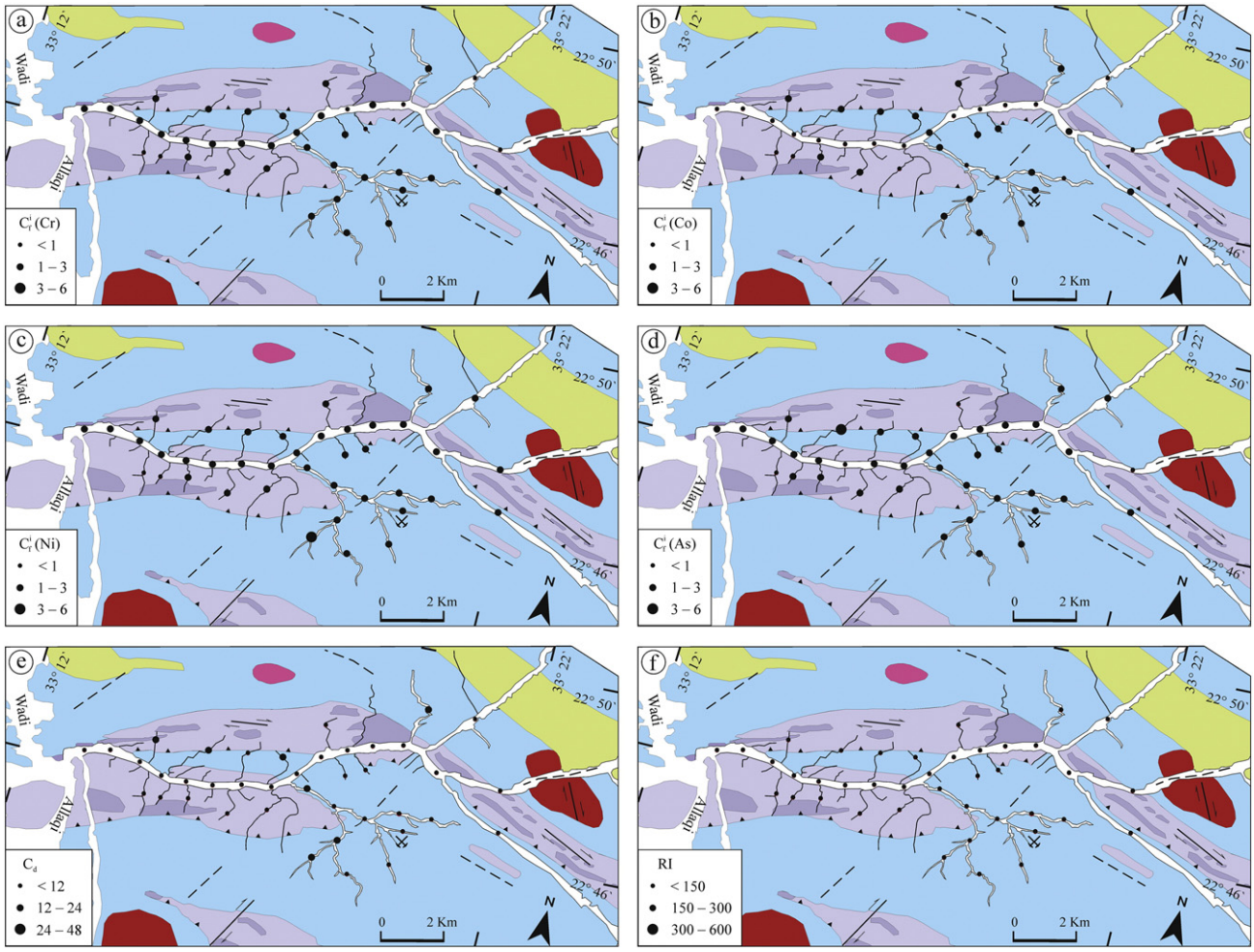

Fig. 9. Ecological geochemical maps of the stream sediments in relation to lithologic units of the Wadi El Quleib area. (a), (b), (c), and (d) contamination factors "C_f^i" of Cr, Co, Ni, and As, respectively, (e) contamination degrees "C_d", and (f) potential ecological risk indices "RI". For lithological units look at Fig. 1.

of Al ($0.8 < rs \geq 0.6$) with Mo, B, Be, Cd and Sr (Table 3). These correlations indicate that the mentioned elements are preferentially incorporated into clay fractions (Lapworth et al., 2012; Šajn et al., 2013). Similarly, most elements in the cluster 6 are very strongly to strongly correlated with Fe and Mn, approving their adsorption onto Fe-and Mn oxide and hydroxide fractions (Lapworth et al., 2012; Papadopoulou-Vrynioti et al., 2013). By the same token, the strong correlation between Ca and Sr is denoting that Sr hosted in the structure of carbonate minerals (Šajn et al., 2013). It cannot be neglected an importance of ferromagnesian minerals, like olivine, pyroxene and hornblende in the mineral assemblage (Lapworth et al., 2012). So that, cluster 6 refers to mineral assemblage; it is generally regarded as lithogenic cluster.

6.6. Principal component analysis

As shown in Table 5, four significant principle components (PCs), whose Eigen values were >1, have been extracted, representing 75.13% of the cumulative variance. By taking only values ±0.5, the first principal component (PC1, 47.04% of total variance) shows the association of Cu, V, Co, Fe, Ti, Mg, Sc, P, Al, Mn, Zn, Cr, Ga, Ni, Mo, Cd, Li, and Sr with its positive loading, and Nb with negative loading, supporting that Nb had different geochemical behavior within the sediments. Majority of these variables exist in cluster 6. The second principal component (PC2, 16.45% of total variance) is defined by the association of Rb, K, Tl, Cs, Pb, La, Ce, Li, Zr, Ba, Sn, Be, Th, Hf, Ga, Y, Mo, and Zn, and is mostly found in cluster 4. The third principal component (PC3, 6.07% of total variance) includes the association of Sr, Hg, and Ca, which are distributed in clusters 2 and 6. The fourth principal component (PC4, 5.56% of total variance) that showed the association of As, Ni, and Cr, is concordant with cluster 5. The negative loading of Na in associations of PC3 and PC4, suggesting that Na has a different behavior rather than those elements in both associations within the environment of stream sediments. The first, second, and third principal components (PC1, PC2, and PC3) are derived from geogenic sources, while the fourth principal component (PC4) is related to both geogenic and anthropogenic sources.

It can be noticed that Ag, Au, Bi, Sb, and U were not grouped within the mentioned four principal components (PCs), because these elements possessed either very low communalities or a tendency to form independent principal component axis. Generally, the principal component analysis is in accordance with the statistical results and interpretation of cluster analysis. Where, both analyses could succeed to define the factors explaining the correlation model between the data variables, assess the degree of association between them and also to exhibit their behavior and possible sources.

6.7. Ecological risk assessment

The calculation of contamination factors reveals two different classes (Table 6 & Fig. 8a): the first class considers the majority of the assessed elements, exhibiting low contamination factor ($C_f^i < 1$). Thereby the stream sediments in the Wadi El Quleib area present total depletion of the most analyzed elements relative to the UCC values; the baseline

levels of these elements cause no dangerous effect upon the sediment materials and thus, do not cause any adverse effects on humans or animals within the area. The second-class corresponding to the remaining four elements: Cr, Co, Ni, and As, which turn to enrichment, and their elevated concentration could cause moderate contamination ($1 < C_f^i < 3$) with mean values of contamination factors equal 1.33, 1.09, 1.65, and 1.49, respectively (Table 6). The order of contaminants based on the elevation of contamination factors can be arranged as follows: Ni > As > Cr > Co. Concerning geochemical patterns of their contamination factors are analogous as shown in Fig. 9a–d. Where, their moderate contamination levels are commonly observed along the tributaries crossing the tectonic contact and those running throughout the drainage sub-basin, including mine waste materials (tailing material heaps) of the newly discovered ancient gold mine. This points to the baseline levels of Cr Co, Ni, and As formed moderate contamination might be influenced by both natural enrichment of geogenic processes and human enrichment of old anthropogenic activities. Both enrichment sources elevated their concentrations and produced an existence of multiple populations in geochemical data. It is reasonable that the mine waste materials, lithology and tectonic zones are possible sources of the stream sediment contamination sourced by Cr Co, Ni, and As.

The contamination degree levels of the more potential toxic heavy metal(loid)s namely, Ti, V, Cr, Mn, Co, Ni, Cu, Zn, Cd, Hg, Pb, and As were assessed using Wisker-plot and geochemical maps (Figs. 8b and 9e). The majority of the sampling stations (82.5%) presents low degrees of contamination ($C_{deg} < 12$), while 17.5% of sampling stations yield the moderate degree of contamination ($12 < C_{deg} < 24$). Based on the mean value of contamination degrees that is < 12 (Table 6 and Fig. 8b), the entire Wadi El Quleib area is generally demonstrated low degree of contamination. Of course, the studied area and its environs are characterized by the absence of major sources of pollution (e.g., agricultural, high-way, rural, urban, and industrial pollution). The environmental geochemical map of contamination degree depicts seven sampling sites influenced by moderate degree of contamination owing to both ancient anthropogenic works for Au and weathering processes. Nevertheless, the potential ecological risk factors for the selected heavy metal(loid)s (Table 6) fall in the division of a low potential ecological risk ($E(i) < 40$) as seen in Fig. 8c. Likewise, the potential ecological risk indices also refer to low ecological risk ($RI < 150$) (Table 6 and Fig. 8d). This is verified by the environmental geochemical map of RI, which exhibits that all sampled stations covering the entire area without exception are low ecological risk (Fig. 9f). Accordingly, the catchment sediments of the study area are not affected by seriously contamination, and free of environmental hazards. They are also good quality and safe because their contents of heavy metal(loid)s may not enter the food chain and the human body, and then did not create a potential risk to human health. Finally, the study area is accepted as the target area for further geochemical exploration and land use purposes in the future.

7. Conclusion

In a light of increased focus on gold exploration and environmental issues in Egypt, the Wadi El Quleib area contained newly discovered ancient gold mine which was chosen. From the present study, it can be concluded that the multiple populations within geochemical data were generated by geologic processes and old anthropogenic enrichment. Non parametric correlation coefficient could assess the relation between the analyzed elements. Although, lithology, tectonic zones and weathering history played significant roles for producing the stream sediments, their generated materials did not follow the sedimentary sorting and recycling trend. The monitored geochemical patterns of Au and Ag are still existed despite streambed sediments were disturbed by former mining activities performed in the past. The multi-element combinations of Ag + As, Ag + Hg and Ag + Hg + As are more important and considered as useful pathfinders for Au-mineralization in the Wadi El Quleib area. Cluster analysis and principal component analysis proved to be a powerful tool for grouping the determined elements based on their geogenic and ancient anthropogenic inputs. It also depicts the mineralogy of the catchment's sediments, and supports the description and interpretation of the geochemical maps. The lateral distribution and mechanism of dispersion of the interesting elements in the catchment basin were controlled by detritus grains and minerals derived from the country rocks, climate besides physical and chemical weathering processes, and old mining activities. It is also concluded that the tectonic zones, metamorphosed ultramafic and their derivatives, and volcanogenic metasediments have hosted Au-mineralization, Cr-mineralization and the Ni-bearing minerals. Environmentally, despite Cr Co, Ni, and As in the stream sediments are related to geogenic sources and ancient human activities, the contamination degrees and potential ecological risk indices of the elements are in the safe range. Over, all the assessed metal(loid)s are not harmful and thus, the sediment materials have no deterioration of their quality, and free of ecological risk. Eventually, the present study is very helpful for effective future mineral exploration, further environmental monitoring, urban renewal purposes and land-use management. Future works should focus on carrying out stream sediments sampling at depth one to three meters and lithogeochemical exploration for Au, especially along thrust contact and drainage sub-basin are recommended in order to define the location of Au mineralization, Ni-bearing minerals and the Cr-mineralization.

References

Abdel Hamid, S.A., 1997. Geology of the Area North Dineibit El-Quleib, South Eastern Desert, Egypt. M.Sc. Thesis. Aswan Faculty of Science, South Valley University, Egypt.

Abdolmaleki, M., Mokhtari, A.R., Akbar, S., Alipour-Asll, M., Carranza, E.J.M., 2014. Catchment basin analysis of stream sediment geochemical data: incorporation of slope effect. J. Geochem. Explor. 140, 96–103.

Ahmed, A.A., 2002. Geological, Petrological, Structural, and Geochemical Studies of the Pan-African Rocks at Wadi El Qulieb Area, South Eastern Desert-Egypt. Ph.D. Thesis. Faculty of Science, Al Azhar University, Cairo, Egypt.

Appleton, J.D., Ridgway, J., 1992. Regional geochemical mapping in developing countries and is application to environmental studies. Appl. Geochem. 2, 103–110.

Beus, A.A., Grigorian, S.V., 1977. Geo-chemical Exploration Methods for Mineral Deposits. Applied Pub. Co., Willmette Illinois (278p).

Bhuiyan, M.A.H., Rahman, M.J.J., Dampare, S.B., Suzuki, S., 2011. Provenance, tectonics and source weathering of modern fluvial sediments of the Brahmaputra–Jamuna River, Bangladesh: inference from geochemistry. J. Geochem. Explor. 111, 113–137.

Briggs, P.L., 1978. Pattern Recognition Applied to Uranium Prospecting Submitted to the Department of Earth and Planetary Sciences. (233pp).

British Geological Survey (BGS), 1990. Regional Geochemical Atlas: Argyll (British Geological Survey).

Caeiro, S., Costa, M.H., Ramos, T.B., 2005. Assessing heavy metal contamination in Sado Estuary sediment: an index analysis approach. Ecol. Indic. 5, 151–169.

Campos Alvarez, N.O., Roser, B.P., 2007. Geochemistry of black shales from the Lower Cretaceous Paja Formation, Eastern Cordillera, Colombia: source weathering, provenance, and tectonic setting. J. S. Am. Earth Sci. 23, 271–289.

Cao, L., Cheng, Q., 2012. Quantification of anisotropic scale invariance of geochemical anomalies associated with Sn-Cu mineralization in Gejiu, Yunan Province, China. J. Geochem. Explor. 122, 47–54.

Castillo-Munoz, R., Howarth, R.J., 1976. Application of the empirical discriminant function to regional geochemical data from the United Kingdom. Geol. Soc. Am. Bull. 87, 1567–1581.

Chandrajith, R., Dissanayake, C.B., Tobschall, H.J., 2001. Application of multi-element relationships in stream sediments to mineral exploration: a case study of Walawe Ganga Basin, Sri Lanka. Appl. Geochem. 16, 339–350.

Chapman, D., 1996. Water Quality Assessments. A Guide to the Use of Biota, Sediments and Water in Environmental Monitoring. Chapman & Hall, London.

Chipres, J.A., Castro-Larragoitia, J., Monroy, M.G., 2009. Exploratory and spatial data analysis (EDA–SDA) for determining regional background levels and anomalies of potentially toxic elements in soils from Catorce–Matehuala, Mexico. Appl. Geochem. 24 (8), 1579–1589.

Christie, T., Fletcher, W.K., 1999. Contamination from forestry activities: implications for stream sediment exploration programmes. J. Geochem. Explor. 67, 201–210.

Church, W.R., 1988. Ophiolites, Sutures, and Microplates of the Arabian Nubian Shield: A Critical Comment.

Cicchella, D., Lima, A., Birke, M., Demetriades, A., Wang, X., De Vivo, B., 2013. Mapping geochemical patterns at regional to continental scales using composite samples to reduce the analytical costs. J. Geochem. Explor. 124, 79–91.

Cohen, D.R., Silva-Santisteban, C.M., Rutherford, N.F., Garnett, D.L., Waldron, H.M., 1999. Comparison of vegetation and stream sediment geochemical patterns in northeastern New South Wales. J. Geochem. Explor. 66, 469–489.

Collyer, P.L., Merriam, D.F., 1973. An application of cluster analysis in mineral exploration. Math. Geol. 4, 213–223.
Condie, K.C., 1993. Chemical composition and evolution of the upper continental crust: contrasting results from surface samples and shales. Chem. Geol. 104, 1–37.
Correll, R.L., 2001. The use of composite sampling in contaminated sites — a case study. Environ. Ecol. Stat. 8, 185–200.
Cox, R., Lowe, D.R., Cullers, R.L., 1995. The influence of sediment recycling and basement composition on evolution of mudrock chemistry in the southwestern United States. Geochim. Cosmochim. Acta 59, 2919–2940.
Crock, J.G., Severson, R.C., Gough, L.P., 1992. Determining baselines and variability of elements in plants and soils near the Kenai national wildlife refuge, Alaska. Water Air Soil Pollut. 63, 253–271.
Cullers, R.L., 1994. The chemical signature of source rocks in size fractions of Holocene stream sediment derived from metamorphic rocks in the Wet Mountains region. USA. Chem. Geol. 113, 327–343.
Darnley, A.G., 1990. International geochemical mapping: a new global project. J. Geochem. Explor. 39, 1–13.
Darnley, A.G., 1997. A global geochemical reference network: the foundation for geochemical baselines. J. Geochem. Explor. 60, 1–5.
Davis, H.T., Aelion, C.M., McDermott, S.Z., Lawson, A.B., 2009. Identifying natural and anthropogenic sources of metals in urban and rural soils using GIS-based data, PCA, and spatial interpolation. Environ. Pollut. 157 (2009), 2378–2385.
Dragovic, S., Mihailovic, N., Gajic, B., 2008. Heavy metals in soils: distribution, relationship with soil characteristics and radionuclides and multivariate assessment of contamination sources. Chemosphere 72, 491–495.
El Afandy, A.H., El Mezayen, A.M., Abdel Rahman, E.M., Ammar, F.A., Ahmed, A.A., 2007. Geological and geochemical studies of the Pan-African rocks at Wadi El Qulieb area, Southeastern Desert. Egypt. J. Fac. Sci. Minufia Uni. XXI, 159–195.
El Baz, A., Nayak, T.K., 2004. Efficiency of composite sampling for estimating a lognormal distribution. Environ. Ecol. Stat. 11, 283–294.
El Shimy, K.M., 1996. Geology, Structure and Exploration of Gold Mineralization in Wadi Allaqi Area SW, Eastern Desert Egypt. Faculty of Science, Ph.D. Thesis. Ain Shams University, Cairo, Egypt.
El-Sayed, M.M., Nisr, S.A., 1999. Petrogenesis and evolution of the Dineibit El-Qulieb hyperaluminous leucogranite, Southeastern Desert, Egypt: petrological and geochemical constraints. J. Afr. Earth Sci. 28 (3), 703–720.
Fawzy, S.M.A., Yousef, M., Ghazaly, M., El Amin, H., Abdel Hamid, S., 2000. Metmorphic imprints of the area north of Denibit El Quleib, S.E.D., Egypt: evidence from metamorphic rocks for overthrusting. Annals Geol. Surv. Egypt. XXIII, 525–538.
Filzmoser, P., Hron, K., Reimann, C., 2009. Univariate statistical analysis of environmental (compositional) data: problems and possibilities. Sci. Total Environ. 407, 6100–6108.
Garrett, R.G., Reimann, C., Smith, D.B., Xie, X., 2008. From geochemical prospecting to international geochemical mapping: an historical overview. Geochem. Explor. Environ. Anal. 8, 205–217.
Guillén, M.T., Delgado, J., Albanese, S., Nieto, J.M., Lima, A., De Vivo, B., 2011. Environmental geochemical mapping of Huelva municipality soils (SW Spain) as a tool to determine background and baseline values. J. Geochem. Explor. 109, 59–69.
Gustavsson, N., Bjorklund, A., 1976. Lithological classification of tills by discriminant analysis. J. Geochem. Explor. 29, 89–103.
Hakånson, L., 1980. An ecological risk index for aquatic pollution control. A sedimentological approach. Water Res. 14 (8), 975–1001.
Hanesch, M., Scholger, R., Dekkers, M.J., 2001. The application of fuzzy c-means cluster analysis and non-linear mapping to a soil data set for the detection of polluted sites. Phys. Chem. Earth, Part A Solid Earth Geod. 26 (11–12), 885–891.
Harnois, L., 1988. The CIW index: a new chemical index of weathering. Sediment. Geol. 55, 319–322.
Harraz, H.Z., Mohamed, M., Hamdy, M.M., Mohamed, H., El-Mamoney, M.H., 2012. Multi-element association analysis of stream sediment geochemistry data for predicting gold deposits in Barramiya gold mine, Eastern Desert, Egypt. J. Afr. Earth Sci. 68, 1–14.
Hossain, I., Roy, K.K., Biswas, P.K., Alam, M., Moniruzzaman, M.D., Deeba, F., 2014. Geochemical characteristics of Holocene sediments from Chuadanga district, Bangladesh: implications for weathering, climate, redox conditions, provenance and tectonic setting. Chin. J. Geochem. 33, 336–350.
Howarth, R.J., 1973. The pattern recognition problem in applied geochemistry. In: Jones, M.J. (Ed.), Geochemical Exploration 1972. Institution of Mining and Metallurgy, London, pp. 259–273.
Johnson, C.C., Breward, N., Ander, E.L., Ault, L., 2005. G-BASE: baseline geochemical mapping of Great Britain and Northern Ireland. Geochem. Explor. Environ. Anal. 5, 347–357.
Kaiser, H.F., 1958. The varimax criterion for analytic rotation in factor analysis. Psychometrika 23, 187–200.
Kalender, L., Uçar, S.Ç., 2013. Assessment of metal contamination in sediments in the tributaries of the Euphrates River, using pollution indices and the determination of the pollution source, Turkey. J. Geochem. Explor. 134, 73–84.
Key, R.M., De Waele, B., Liyungu, A.K., 2004. A multi-element baseline geochemical database from the western extension of the Central African Copperbelt in north western Zambia. Trans. Inst. Min. Metall. B Appl. Earth Sci. 113, 205–226.
Khalil, A., Hanich, L., Bannari, A., Zouhri, L., Pourret, O., Hakkou, R., 2013. Assessment of soil contamination around an abandoned mine in a semi-arid environment using geochemistry and geostatistics: pre-work of geochemical process modeling with numerical models. J. Geochem. Explor. 125, 117–129.
Lapworth, D.J., Knights, K.V., Key, R.M., Johnson, C.C., Ayoade, E., Adekanmi, M.A., Arisekola, T.M., Okunlola, O.A., Backman, B., Eklund, M., Everett, P.A., Lister, R.T., Ridgway, J., Watts, M.J., Kemp, S.J., Pitfield, P.E.J., 2012. Geochemical mapping using stream sediments in west-central Nigeria: implications for environmental studies and mineral exploration in West Africa. Appl. Geochem. 27, 1035–1052.
Li, Z.G., Feng, X.B., Li, G.H., Bi, X.Y., Sun, G.Y., Zhu, J.M., Qin, H.B., Wang, J.X., 2011. Mercury and other metal and metalloid soil contamination near a Pb/Zn smelter in east east Hunan province, China. Appl. Geochem. 26, 160–166.
Lin, X., Wang, X., Zhang, B., Yao, W., 2014. Multivariate analysis of regolith sediment geochemical data from the Jinwozi gold field, north-western China. J. Geochem. Explor. 137, 48–54.
Lu, X.W., Wang, L.J., Li, L.Y., Lei, K., Huang, L., Kang, D., 2010. Multivariate statistical analysis of heavy metals in street dust of Baoji, NW China. J. Hazard. Mater. 173, 744–749.
Manta, D.S., Angelone, M., Bellanca, A., Neri, R., Sprovieri, M., 2002. Heavy metals in urban soils: a case study from the city of Palermo (Sicily), Italy. Sci. Total Environ. 30, 229–243.
Martínez, J., Llamas, J., de Miguel, E., Rey, J., Hidalgo, M.C., 2007. Determination of the geochemical background in a metal mining site: example of the mining district of Linares (South Spain). J. Geochem. Explor. 94, 19–29.
McLennan, S.M., 1993. Weathering and global denudation. J. Geol. 101, 295–303.
McLennan, S.M., Taylor, S.R., 1991. Sedimentary rocks and crustal evolution: tectonic setting and secular trends. J. Geol. 99, 1–21.
McLennan, S.M., Hemming, S., McDaniel, D.K., Hanson, G.N., 1993. Geochemical approach to sedimentation, provenance, and tectonics. Spec. Pap.-Geol. Soc. Am. 284, 21–40.
Moreno, T., Querol, X., Castillo, S., Alastuey, A., Cuevas, E., Herrmann, L., Mounkaila, M., Elvira, J., Gibbons, W., 2006. Geochemical variations in aeolian mineral particles from the Sahara–Sahel Dust Corridor. Chemosphere 65 (2), 261–270.
Navas, A., Machĭn, J., 2002. Spatial distribution of heavy metals and arsenic in soils of Aragón (northeast Spain): controlling factors and environmental implications. Appl. Geochem. 17, 961–973.
Nesbitt, H.W., Young, G.M., 1982. Early Proterozoic climates and plate motions inferred from major element chemistry of lutites. Nature 299, 715–717.
Nesbitt, H.W., Young, G.M., 1984. Prediction of some weathering trends of plutonic and volcanic rocks based on thermodynamic and kinetic considerations. Geochim. Cosmochim. Acta 48, 1523–1534.
Nesbitt, H.W., Young, G.M., 1989. Formation and diagenesis of weathering profiles. J. Geol. 97, 129–147.
Nesbitt, H.W., Markovics, G., Price, R.C., 1980. Chemical processes affecting alkalis and alkaline earths during continental weathering. Geochim. Cosmochim. Acta 44, 1659–1666.
Nesbitt, H.W., Young, G.M., McLennan, S.M., Keays, R.R., 1996. Effects of chemical weathering and sorting on the petrogenesis of siliciclastic sediments, with implication for provenance studies. J. Geol. 104, 525–542.
Nesbitt, H.W., Fedo, C.M., Young, G.G., 1997. Quartz and feldspar stability, steady and non-steady-state weathering, and petrogenesis of siliciclastic sands and muds. J. Geol. 105, 173–191.
Nockolds, S.R., 1954. Average chemical compositions of some igneous rocks. J. Geol. Soc. Am. Bull. 65, 1007–1032.
Noweir, A.M., El Amawy, M.A., 1999. Geochemistry, metamorphic aureole and structural analysis of Deneibit El Quleib granite pluton and its environ, Wadi Allaqi district, south Eastern Desert. Egypt. Annals Geol. Surv. Egypt XXII, 27–45.
Noweir, A.M., Rashwan, A.A., Abu El Ela, A.M., El Hashash, M.A.A., 2000. Petrology, petrochemistry and crustal evolution of the PreCambrian rocks, Wadi Umm Ashira, south Eastern Desert, Egypt. Annals Geol. Surv. Egypt. XXIII 961–981.
Ohta, A., Imai, N., Terashima, S., Tachibana, Y., 2005. Application of multi-element statistical analysis for regional geochemical mapping in Central Japan. Appl. Geochem. 20, 1017–1037.
Ohta, A., Imai, N., Terashima, S., Tachibana, Y., Ikehara, K., Okai, T., Ujiie-Mikoshiba, M., Kubota, R., 2007. Elemental distribution of coastal sea and stream sediments in the island-arc region of Japan and mass transfer processes from terrestrial to marine environments. Appl. Geochem. 22, 2872–2891.
Papadopoulou-Vrynioti, K., Alexakis, D., Bathrellos, G.D., Skilodimou, H.D., Vryniotis, D., Vassiliades, E., Gamvroula, D., 2013. Distribution of trace elements in stream sediments of Arta plain (western Hellas): the influence of geomorphological parameters. J. Geochem. Explor. 134, 17–26.
Pekey, H., Karakaş, D., Ayberk, S., et al., 2004. Ecological risk assessment using trace elements from surface sediments of İzmit Bay (Northeastern Marmara Sea) Turkey. Mar. Pollut. Bull. 48, 946–953.
Plant, J.A., Smith, D., Smith, B., Williams, L., 2000. Environmental geochemistry at the global scale. J. Geol. Soc. Lond. 157, 837–849.
Plant, J.A., Smith, D., Smith, B., Williams, L., 2001. Environmental geochemistry at the global scale. Appl. Geochem. 16, 1291–1308.
Plant, J.A., Reeder, S., Salminen, R., Smith, D.B., Tarvainen, T., De Vivo, B., Petterson, M.G., 2003. The distribution of uranium over Europe: geological and environmental significance. Appl. Earth Sci. 112, 221–238.
Pohl, J.R., Emmermann, R., 1991. Chemical Composition of the Sri Lankan Precambrian Basements. Crystalline Crust of Sri Lanka (Part 1), Professional Paper No. 5. Geological Survey and Mines Bureau, Sri Lanka.
Ragab, A.G.I., El Shimy, K.A., 1994. On the origin of volcanogenic foreland molasse sediments in Wadi Allaqi, South Eastern desert, Egypt. 32th Annu. Meet. Geol. Soc. Egypt. Abstr, p. 1.
Rashawan, A.A., Schleicher, H., 1996. Contrasting geochemical trends of some granitic rocks from the Eastern Desert, Egypt. Centennial Geol. Surv. Egypt. Abstr. 158–159 Cairo, Egypt 19–22 Nov..
Reimann, C., Ayras, M., Chekushin, V., Bogatyrev, I., Boyd, R., de Caaritat, P., Dutter, R., Finne, T.E., Halleraker, J.H., Jager, O., Kashulina, G., Lehto, O., Niskavaara, H., Pavlov, V., Raisanen, M.L., Strand, T., Volden, T., 1998. Environmental Geochemical Atlas of the Central Barents Region (Geological Survey of Norway).
Reimann, C., Filzmoser, P., Garrett, R.G., 2005. Background and threshold: critical comparison of methods of determination. Sci. Total Environ. 346, 1–16.

Reimann, C., Demetriades, A., Eggen, O.A., Filzmoser, P., 2011. The EuroGeoSurveys geochemical mapping of agricultural and grazing land soils (GEMAS). NGU Rpt 043, 2011.
Reimann, C., Filzmoser, P., Fabian, K., Hron, K., Birke, M., Demetriades, A., Dinelli, E., Ladenberger, A., the GEMAS Project Team, 2012. The concept of compositional data analysis in practice—total major element concentrations in agricultural and grazing land soils of Europe. Sci. Total Environ. 426, 196–210.
Reis, A.P., Sousa, A.J., Cardoso, F.E., 2001. Soil geochemical prospecting for gold st Marrancos (North Portugal). J. Geochem. Explor. 73, 1–10.
Rice, K.C., 1999. Trace-element concentrations in streambed sediment across the conterminous United States. Environ. Sci. Technol. 33, 2499–2504.
Šajn, R., Aliu, M., Stafilov, T., Alijagić, J., 2013. Heavy metal contamination of topsoil around a lead and zinc smelter in Kosovska Mitrovica/Mitrovicë, Kosovo/Kosovë. J. Geochem. Explor. 134, 1–16.
Saleh, G.M., Abd El Wahed, A.A., 2001. Pan African granitoid rocks from the Arabian Nubian Shield, SE of Aswan, Egypt: geology, geochemistry and radio activities. Egypt. J. Geol. 45 (1), 169–185.
Salminen, R., Batista, M.J., Bidovec, M., Demetriades, A., De Vivo, B., De Vos, W., Duris, M., Gilucis, A., Gregorauskiene, V., Halamic, J., Heitzmann, P., Lima, A., Jordan, G., Klaver, G., Klein, P., Lis, J., Locutura, J., Marsina, K., Mazreku, A., O'Connor, P.J., Olsson, S.A., Ottesen, R.-T., Petersell, V., Plant, J.A., Reeder, S., Salpeteur, I., Sandstrom, H., Siewers, U., Steenfelt, A., Tarvainen, T., 2005. Geochemical atlas of Europe. Part 1—Background Information, Methodology and Maps. Espoo, Finland, Geological Survey of Finland.
Smith, D.B., Reimann, C., 2008. Low-density geochemical mapping and the robustness of geochemical patterns. Geochem. Explor. Environ. Anal. 8, 219–227.
Splitstone, D.E., 2001. Sample support and related scale issues in composite sampling. Environ. Ecol. Stat. 8, 137–149.
Sun, S.S., Mcdonough, W.F., 1989. Chemical and isotopic systematics of oceanic basalts: Implications for mantle composition and processes. In: Saunders, A.D., Norry, M.J. (Eds.), Magmatism in the Ocean Basins. J. Geol. Soc. Lond. 42. Special Publication, pp. 315–345.
Tan, J., 1989. The Atlas of Endemic Diseases and Their Environments in the People's Republic of China. Science Press, Beijing.
Taylor, S.R., McLennan, S.M., 1985. The Continental Crust: Its Composition and Evolution. Blackwell Scientific Publications, Oxford (312 pp).
Taylor, S.R., McLennan, S.M., 1995. The geochemical evolution of the continental crust. Rev. Geophys. 33, 165–241.
van Helvoort, P.J., Filzmoser, P., van Gaans, P.F.M., 2005. Sequential factor analysis as a new approach to multivariate analysis of heterogeneous geochemical datasets: an application to a bulk chemical characterization of fluvial deposits (Rhine–Meuse delta, The Netherlands). Appl. Geochem. 20, 2233–2251.
Wronkiewicz, D.J., Condie, K.C., 1987. Geochemistry of Archean shales from the Witwatersrand Supergroup, South Africa: source-area weathering and provenance. Geochim. Cosmochim. Acta 51, 2401–2416.
Wu, W.H., Xu, S.J., Yang, J.D., Lu, H.Y., Yin, H.W., Liu, W., 2011. Mineralogy, major and trace element geochemistry of riverbed sediments in the headwaters of the Yangtze, Tongtian River and Jinsha River. J. Asian Earth Sci. 40, 611–621.
Xie, X., Liu, D., Xiang, Y., Yan, G., Lian, C., 2004. Geochemical blocks for predicting large ore deposits-concept and methodology. J. Geochem. Explor. 84, 77–91.
Xu, Z.Q., Ni, S.J., Tuo, X.G., Zhang, C.J., 2008. Calculation of heavy metals' toxicity coefficient in the evaluation of potential ecological risk index. Environ. Sci. Technol. 31, 112–115.
Xuejing, X., Binchuan, Y., 1993. Geochemical pattern from local to global. J. Geochem. Explor. 47, 109–129.
Zhang, C., Wang, L., 2001. Multi element geochemistry of sediments from Pearl River System. China. App. Geochem. 16, 1251–1259.
Zhang, C., Manheim, F.T., Hinde, J., Grossman, J.N., 2005. Statistical characterization of a large geochemical database and effect of sample size. Appl. Geochem. 20, 1857–1874.
Zhou, X., Xia, B., 2010. Defining and modeling the soil geochemical background of heavy metals from the Hengshi River watershed (southern China): integrating EDA, stochastic simulation and magnetic parameters. J. Hazard. Mater. 180, 542–551.